

North Carolina Agricultural and Technical State University
Aggie Digital Collections and Scholarship

Theses

Electronic Theses and Dissertations

2014

Design And Fabrication Of Nanodevice For Cell Interfacing

Prema Chinnappan

North Carolina Agricultural and Technical State University

Follow this and additional works at: <https://digital.library.ncat.edu/theses>

Recommended Citation

Chinnappan, Prema, "Design And Fabrication Of Nanodevice For Cell Interfacing" (2014). *Theses*. 154.
<https://digital.library.ncat.edu/theses/154>

This Thesis is brought to you for free and open access by the Electronic Theses and Dissertations at Aggie Digital Collections and Scholarship. It has been accepted for inclusion in Theses by an authorized administrator of Aggie Digital Collections and Scholarship. For more information, please contact iyanna@ncat.edu.

Design and Fabrication of Nanodevice for Cell Interfacing

Prema Chinnappan

North Carolina A&T State University

A thesis submitted to the graduate faculty
in partial fulfillment of the requirements for the degree of

MASTER OF SCIENCE

Department: Nanoengineering

Major: Nanoengineering

Major Professor: Dr. Shyam Aravamudhan

Greensboro, North Carolina

2014

The Graduate School
North Carolina Agricultural and Technical State University
This is to certify that the Master's Thesis of

Prema Chinnappan

has met the thesis requirements of
North Carolina Agricultural and Technical State University

Greensboro, North Carolina
2014

Approved by:

Dr. Shyam Aravamudhan
Major Professor

Dr. Shanthi Iyer
Committee Member

Dr. Albert Hung
Committee Member

Dr. Jun Yan
Committee Member

Dr. Ajit Kelkar
Department Chair

Dr. Sanjiv Sarin
Dean, The Graduate School

© Copyright by
Prema Chinnappan
2014

Biographical Sketch

Prema Chinnappan got her bachelor's degree in Electronics and Communication Engineering from Amrita Institute of Technology and Science, Bharathiar University, India. After that, she worked in IT industry in various domains like Systems programming, System administration, Networking and Databases. She joined North Carolina A&T State University, Joint School of Nanoscience and Nanoengineering to pursue her Masters in Nanoengineering. Under the supervision of Dr. Shyam Aravamudhan, She did her research in understanding the cell interfacing over nanofins.

Dedication

I dedicate this thesis to my husband Arul.

Acknowledgments

Foremost, I would like to express my sincere gratitude to my advisor Dr. Shyam Aravamudhan for his academic guidance and continuous support of study and research. I thank my committee members Dr. Jun Yan, Dr. Shanthi Iyer and Dr. Albert Hung for their valuable inputs. I would like to acknowledge Dr. James Ryan and Dr. Ajit Kelkar for giving me the great opportunity. I would also like to thank Smith, Karshak, Komal, Sara and everyone in Bio electronics group for their continued support and encouragement. Finally, I like to thank my family and friends.

Table of Contents

List of Figures	x
List of Tables	xiv
Abstract	1
CHAPTER 1 Introduction.....	2
1.1 Objective.....	2
1.2 Motivation.....	3
1.3 Thesis Outline.....	4
CHAPTER 2 Literature Review	5
2.1 Structure of Neuron	5
2.2 Action Potential	6
2.3 Intracellular and Extracellular Recording.....	6
CHAPTER 3 Design and Fabrication of Nanofin Device	9
3.1 Design of the Device	9
3.1.1 Equivalent circuit.....	9
3.2 Fabrication of the Device.....	12
3.2.1 Optimization of the FIB process.....	12
3.2.2 Optimization to find clear cut lines.	13
3.2.3 Optimization to find the pitch – drawing parallel vertical and horizontal lines....	14
3.2.4 Effect of dosage and current on milling distance.	14
3.2.5 FIB first SOI process flow.....	16
3.2.6 EBL process flow.	17
3.2.6.1 Optimization of high density nanofins.	19
3.2.7 SOI based design.	23

3.2.7.1 Optimization of low density nanofins.	24
3.2.7.2 Optimization up to 200 nm.....	26
CHAPTER 4 Growing Cells over Nanofins	31
4.1 Cell Lines.....	31
4.2 Optimization of Adherence Protocol of PC12 Cells over Au Nanofins	32
4.2.1 Adherence by physisorption.	32
4.2.1.1 Experiments with collagen.	33
4.2.2 Adherence by physisorption and chemisorption.	33
4.2.2.1 SAM formation.	34
4.2.2.2 Cross linking.	34
4.2.2.3 Experiments with PDL.	34
4.2.2.3.1 Contact angle measurement.	40
4.3 Cell Culturing over Nanofins.....	42
4.4 Differentiation Experiments	47
4.5 Preliminary Impedance Measurement	49
CHAPTER 5 Discussion and Future Research.....	51
5.1 Device Fabrication.....	51
5.2 Nanofin Fabrication	52
5.3 Cell Culture over Nanofins	52
5.4 Immobilization of Cells over Gold Surfaces	54
5.5 Differentiation.....	54
5.6 Future Research	55

References.....	56
Appendix A.....	59
Appendix B.....	64
Appendix C.....	65
Appendix D.....	66

List of Figures

Figure 2.1. Structure of neuron (Carlson, 2005).....	5
Figure 2.2. Vertical nanoelectrode arrays (Robinson et al., 2012).	7
Figure 2.3. Mushroom shaped electrode (Spira & Hai, 2013).....	8
Figure 2.4. Kinked probe (Xie & Cui, 2010).....	8
Figure 3.1. Equivalent circuit showing electrode cytosol contact.	10
Figure 3.2. Equivalent circuit showing no electrode cytosol contact.	11
Figure 3.3. Shows conventional nanopillar design to nanofin.....	12
Figure 3.4. Comparison of dimensions of nanopillars with nanofins.	12
Figure 3.5. Optimization to find clear cut lines: a) Lines in various currents and dosages; b) 2 nA current with 5nC, 10nC and 15 nC dosage from left to right; c) Observation of depth of a vertical line; d) Milling to find the width of the vertical line.	13
Figure 3.6. Optimization of pitch: a) Parallel vertical lines; b) Parallel horizontal lines and vertical lines.....	14
Figure 3.7. Milled lines to show different depths in different dosages.....	14
Figure 3.8. Milling done on different dosages: a) 1nC; b) 2nC; c) 5nC.....	15
Figure 3.9. Effect of dosage on milling distance and time: a) Dosage vs Distance milled; b) Dosage vs Time.....	16
Figure 3.10. Schematic representation of FIB first SOI based design.....	17
Figure 3.11. Schematic representation of EBL process flow.....	18
Figure 3.12. Horizontal lines shifting to the left.	19
Figure 3.13. Position of the cut: a) Milling done in trough instead of the crest; b) Deeper ridge was cut to observe the details.....	19

Figure 3.14. High density nanofins: a) Aligned horizontal lines; b) Nanofin structure.	20
Figure 3.15. Nanofins after electron beam lithography: a) Bubbles showing the hardened region; b) Squared region showing the nanofins.....	20
Figure 3.16. Nanofins after dosage optimization: a) Nanofins after showing e-beam; b) Two nanofins with 0.2 nC dosage.	22
Figure 3.17. Schematic representation of SOI based design.	23
Figure 3.18. Intermediate steps in the SOI process flow: a) After developing by MF-321; b) After oxide etch by BOE; c) After Si etch by KOH.....	23
Figure 3.19. Optimization of current: a) Specification for 4 by 4 μm squares; b) 4 by 4 μm squares with 12 nA 10nc; c) Nanofins with various currents and dosages; d) 300 nm nanofins.	24
Figure 3.20. Device: a) Contact pad and track lines; b) Device with contact pads and conducting wire.	25
Figure 3.21. Optimization of nanofins up to 200 nm: a) Width optimization; b) 200 nm width nanofins; c) Width optimization; d)200 nm width nanofins; e)Placement chamber after height optimization; f)200 nm width ,1 μm height nanofins.	26
Figure 3.22. Changes during the process flow: a) Open track lines; b) Oxidation details; c) Photo resist not removed with acetone and IPA; d) Fins eroded after treating with piranha.....	27
Figure 3.23. Gold coating over the milled region: a) Gold in the milled area of the contact pad; b) Gold over the nanofins.....	28
Figure 4.1. PC 12 cells adhered over the collagen coated Si substrate.....	33
Figure 4.2. Collagen covering the nanofins.	33
Figure 4.3. PDL experiments for cell adherence: a) 120 nm + lipoic acid +PDL; b) 120 nm +PDL; c) 20 nm +lipoic acid +PDL; d) 20 nm +PDL; e) 120 nm +PDL after 96 hours.....	36

Figure 4.4. Comparing the adherence between PDL and cysteamine: a) PDL; b) cysteamine+EDC NHS+PDL.	39
Figure 4.5. Contact angle measurements of the intermediate steps of functionalization.	40
Figure 4.6. Cell adherence after 3 days: a) L-cysteine +EDC NHS +PDL; b) L-cysteine +PDL; c) MPA +EDC NHS +PDL; d) MPA + PDL.	41
Figure 4.7. Cell adherence after 5 days: a) L-cysteine +PDL; b) L-cysteine+ EDC NHS +PDL;	42
Figure 4.8. ZEISS Z2M upright microscope images of PC 12 cells: a) over nanofins with 5X magnification; b) Over nanofins with 10X magnification c) Over nanofins of 1 μ m x 1 μ m area with 10X magnification; d) Over nanofins of 1 μ m x 1 μ m area with 20X magnification.	43
Figure 4.9. EVO SEM images of PC 12 cells over the nanofins: a) Cells over nanofins; b) Magnified image of cells over nanofins.	43
Figure 4.10. SEM images of cell over the track: a) Cell near the nanofins; c) Cell over the track line.	44
Figure 4.11. SEM images of cell near the track a) Cell near the ridges of the track b) Cell on the edge of the large lines.	45
Figure 4.12. Adhered cell over high density nanofins: a) Cell over the pillars; b) Cell over the nanofins.	46
Figure 4.13. SEM images: a) Gold peeling b) Displaced nanofins.	46
Figure 4.14. Adhered cells over low density nanofins: a) Placement chamber; b) Cell over the placement chamber.	47
Figure 4.15. Differentiated PC12 cells: a) 20X magnification b) 40X magnification.	47
Figure 4.16. Cell adherence on 1st day.	48
Figure 4.17. Differentiation on: a) 3 rd day; b) 5 th day; c) 6 th day; d) 6 th day of adding NGF.	49

Figure 4.18. Device setup for impedance measurement: a) Device with output taken from the contact pads by conducting glue and copper wire b) Device and the sealed well.	50
Figure 4.19. Impedance measurement.	50
Figure 5.1. Device with contact pad and track lines.	51
Figure 5.2. Nanofin structures with a) 10 nC; b) 5 nC; c) 10 nC Dosages.	52
Figure 5.3. Cell cultured over high density a) Pillars; b) Nanofins.	53
Figure 5.4. Cell cultured over high density nanofins : a) Placement chamber; b) Cell adhered over nanofins.	53
Figure 5.5. Adherence of PC12 cells by chemisorption: a) L-cysteine+ EDC NHS +PDL; b) MPA+EDC NHS+PDL.	54
Figure 5.6. Differentiation of PC12 cells.	54

List of Tables

Table 3.1. Optimization of e-beam dosage.	21
Table 3.2. Nanofin structure in five of the track lines over the device.	29
Table 4.1. Six well plate combinations of MPA, L-cysteine	41
Table 4.2. Combination of NGF Concentration in ng/ml	48

Abstract

The goal of this thesis is to (a) design and fabricate a nanodevice that interface with cells and (b) optimize neuronal cell culturing protocol. The long term objective of this thesis is to perform intracellular electrical signal recording and stimulation of neuronal cells. To achieve this objective, a nanodevice with “Fin” shaped electrodes was designed that increases the electrode area and conductance so that it reduces the signal loss as shown in the case of traditional circular Nanopillar design. The overarching goal of neuroscience is to target and discover the relationships between the functional connectivity-map of neuronal circuits and their physiological or pathological functions. For recording large number of neurons, technologies such as gold mushroom-shaped microelectrodes (Hai et al.), vertical nanowire electrode arrays (VNEAs) (Robinson et al.) and nanoFET technology (Tian et al.) are currently under development. The gold mushroom-shaped electrodes in order of microns are invasive for smaller cells with no successful recording for long durations. The VNEAs show high electrode impedance which causes large signal loss. The nanoFET shows higher noise levels and the manipulation of a single nanotube to penetrate a single cell is very challenging. This thesis presents the design and fabrication of a “Fin” shaped nanoelectrode which seeks to overcome the restrictions between electrode impedance and electrode size. Compared to the 3x3 array of 200nm diameter nanowire electrodes, the “Fin” electrodes reduces the interfacial impedance. The fabrication was done in Silicon on insulator wafer with conducting lines and contact pads completely insulated by Silicon dioxide layer and gold coated nanofins. Nanofins of width 200 nm were fabricated using Focused Ion Beam (FIB) milling. Both high density and low density nanofins were optimized and cells were cultured over them. The optimization of cell culture, adherence and differentiation protocols were done to grow cells over the nanofins.

CHAPTER 1

Introduction

1.1 Objective

The main objective of this research was to design and fabricate a nanofin device fabricated by Focused Ion Beam (FIB) milling for cell interfacing. Also, for interfacing the cells over the nanofins, the goal was to optimize cell culture, adherence and differentiation protocols.

The specific objectives of this research were to:

- a) Design and fabricate a nanodevice with nanofins up to 200 nm width
- b) Optimize the adherence and differentiation protocol for PC12 cells
- c) Optimize placement, culturing and growth of the cells over the nanofins.

The long term goal is to record intracellular neuronal recordings. Extracellular recordings are less invasive and simultaneous recording of large population of neuronal cells are possible for longer durations. Extracellular field potential is the combination of fast Action Potentials (APs), synaptic potentials and slow glial potentials. Even though, lot of information is gained through these extracellular field potential, the information in spike pattern is limited. The extensive spike sorting cannot provide information such as actual firing of neuron whether it may be due to endogenous mechanism, incoming inhibition or excitatory signal or the combination, the ending of the firing mechanism. Also, the dark neurons that do not fire APs during the recording time are entirely missed during the extracellular recording. But the intracellular recordings can provide considerable information regarding the silent majority of dark neurons. Intracellular recordings measure the action potential as well as the sub synaptic field potential (Hai, Shappir, & Spira, 2010; Yuste, 2008).

1.2 Motivation

The last thing a human mind can design and implement is the artificial brain because of the complexity of its functioning. Understanding the physiology and functioning of the neurons is the smallest step closer towards this ultimate challenge. Measuring the action potential and sub-threshold synaptic potential can help to get insights into firing of these potentials and how the information is transmitted via neurons.

At present, the widely used method for analyzing the connectivity of neuronal circuits, physiology and pathology under *in vitro* or *in vivo* conditions is by using substrate-integrated microelectrode arrays. Although this method permits simultaneous, cell-non-invasive, long-term recordings of extracellular field potentials generated by action potentials, it cannot measure the sub-threshold synaptic potentials generated by single cells. But, intracellular recordings of the full electrophysiological parameters like sub-threshold synaptic potentials; membrane oscillations and action potentials are, at present, obtained only by sharp or patch microelectrodes. These, however, are limited to single cells at a time and for short durations. Recently, lot of research is being done to merge the advantages of extracellular microelectrode arrays and intracellular nanoelectrode (Spira & Hai, 2013).

Thus, one of the merits of the proposed research is that the successful nanofin neuronal interfacing combines the benefits of intracellular as well as extracellular recording to simultaneously measure and control large number of mammalian neurons with single-cell resolution. This method can be used for the pharmacological screening of ion channel in drugs. Also, one other advantage and inspiration of this research is that the understanding of the functions of the neuronal circuits as well as the ion channel studies in drugs can result in the

effective clinical treatment of many neurological conditions like Parkinson's disease, Alzheimer's disease (Xie & Cui, 2010).

1.3 Thesis Outline

This chapter introduces the objective of this research. Chapter 2 presents a brief literature review, summary of intracellular and extracellular recordings and the recent trends in benefits of combining them. Chapter 3 explains the design and fabrication of the device. Chapter 4 explains the cell culture and placement of cell over nanofins. Chapter 5 discusses the results and future prospects of this research.

CHAPTER 2

Literature Review

2.1 Structure of Neuron

Neurons are the excitable cells in the nervous system that process and transmit information. The structure of the neuron is well established and for the understanding of action potential, it is important to know the role of each component in the neuron. The main parts of the neurons are Dendrites, Soma, axons and the terminal buttons or synapses. Soma or cell body consists of cell machinery that provides for the life processes of the cell like nucleus, mitochondria etc. It is responsible for the synthesis of neurotransmitters. Dendrites of the neurons look like trees. When neurons talk to each other dendrites receive the messages. Axon transmits the messages i.e. the action potential from the soma to the terminal buttons. They are usually covered by myelin sheath (Carlson, 2005).

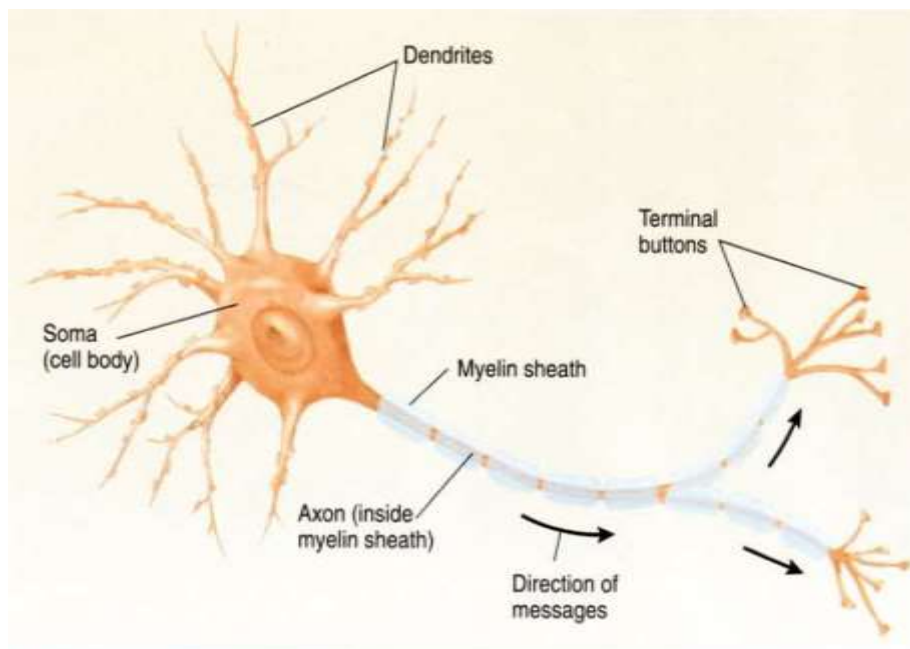


Figure 2.1. Structure of neuron (Carlson, 2005).

2.2 Action Potential

The flow of ions in and out of the neuron's cell membrane changes the membrane potential. If this potential is above the threshold voltage, action potential is fired. The resting potential of PC12 cells grown in the presence or absence of NGF (Nerve Growth Factor) ranged from -35 to -60 mV. No significant differences are found on the basis of whether the cells were grown in the presence or absence of NGF. Amplitude of the action potential increases up to 30 mV from the resting potential (Rudy, Kirschenbaum, & Greene, 1982). Action Potential is generated in the axon in the region where it is connected to the cell body. AP travels down the axon and when it reaches synapses, neurotransmitters are released.

The voltage difference inside is negative with respect to outside of the neuron. Cations like Na^+ and K^+ anions like Cl^- and protein anions in the membrane play a significant part. The ions move in and out either by means of passive transport or active transport. In active transport, the proteins in the cell opens and closes like a faucet and flows from higher to lower concentration. In active transport the cell uses some of its energy to pump ions against the gradient. Generally it pumps 3 Na^+ ions out and 2 K^+ ions in. So totally the potential is negative inside the cell (Kandel, Schwartz, & Jessell, 2000).

Recording the action potential and sub synaptic potential with respect to intracellular and extracellular recording is reviewed in the next section.

2.3 Intracellular and Extracellular Recording

Planar Multi Electrode Arrays (MEAs) were the traditional tools used for extracellular recordings from cultured cells. In 1972 Thomas et al developed an array which had two rows of 15 electrodes each spaced 100 μm to record the signals from cultured dorsal root ganglion neurons. But the attempt was unsuccessful due to the confluent glial layer that insulated the

neurons from their electrodes (Thomas, Springer, Loeb, Berwald-Netter, & Okun, 1972). Pine et al reported the first successful recordings from single dissociated neurons from MEAs which consists of 16 gold electrodes, platinized and had silicon dioxide as insulator (Pine, 1980). Jobling et al reported 9 Field Effect Transistor (FET) transistor electrodes on a silicon chip with effective recordings from hippocampal slices .They demonstrated good signal to noise ratio (Jobling, Smith, & Wheal, 1981). Taketani and Kawana fabricated 64 electrode MEAs over which rat cortical neurons are grown and they observed that the stimulation of one electrode affected all the neurons. Silicon nanowire transistors were fabricated and they acted as electrodes and the extracellular potentials of cardiac cells of HL-1 cell lines were recorded. They had a better signal to noise ratio as compared to the planar FET device (Eschermann et al., 2009). Kipke et al had shown that extracellular MEAs can record spikes in vivo for three months and more (Kipke, Vetter, Williams, & Hetke, 2003).

Lately, Martina et al had shown successful synaptic activity detection using microfluidic patch clamps (Martina et al., 2011). Advances in nanofabrication have paved the way for accurate biological measurements using nanoelectrodes (Yeh & Shi, 2010). For simultaneous recording of large number of neurons, currently lot of work is being done. Park et al are developing VNEAs which has vertical nanopillars penetrating the neurons for intracellular recording (Robinson et al., 2012).

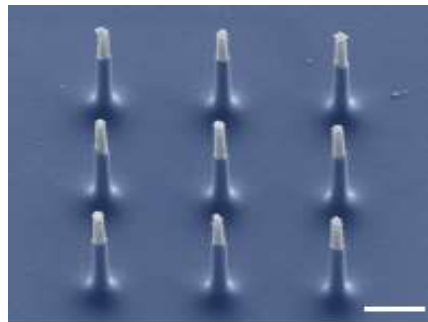


Figure 2.2. Vertical nanoelectrode arrays (Robinson et al., 2012).

Hai et al have mushroom shaped extracellular electrode just engulfing the neurons but still be able to record intracellular level sub synaptic readings (Hai et al., 2010).

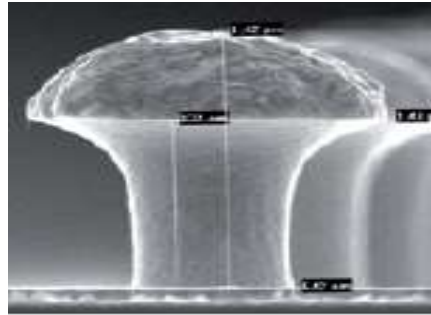


Figure 2.3. Mushroom shaped electrode (Spira & Hai, 2013).

Cui et al are doing nanopillar electroporation for intracellular recording and ion channel studies (Xie & Cui, 2010).

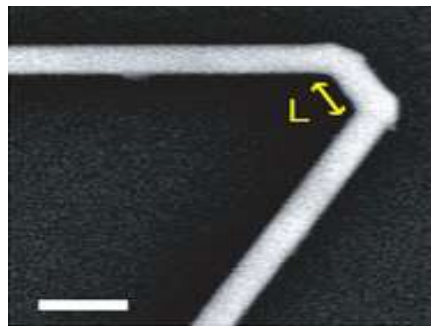


Figure 2.4. Kinked probe (Xie & Cui, 2010).

The vertical nano arrays have high interfacial impedance and electrode resistance so there is large signal loss. Hai's mushroom-shaped electrodes in the order of microns were invasive for smaller cells and also no successful recording for long time on rat hippocampal neurons and primary rat cardiomyocytes. The nanoFET show higher noise levels and the manipulation of a single nanotube to penetrate a single cell are very challenging. In this thesis, the design of the device consists of fin shaped nanoelectrodes, which has higher surface area and hence larger contact with the cells. The chance for making the interface is more and hence lesser interfacial impedance.

CHAPTER 3

Design and Fabrication of Nanofin Device

This thesis research is divided into two main parts as below.

- 1) Design and fabrication of the nanofin device.
- 2) Growing cells over the nanofins.

3.1 Design of the Device

3.1.1 Equivalent circuit. AP is fired when neurotransmitters open passive transport allowing ions to move in and out of the neuron that changes the potential across the cell. This can be modeled using a battery and a resistor. Battery represents the stored potential that is maintained by the Na/K ion pumps and the resistor represents the quantity of ions that are allowed to flow in and out of the cell. Passive transport is represented by the variable resistor. Capacitor represents the Charge separation that is maintained across the cell membrane. Separation of charge by the insulating material causes a capacitive effect on the cell membrane.

If voltage is applied to the circuit, the capacitor stores electricity, eventually it reaches its maximum storage capacity and simply stays there. Once the external voltage is removed, the capacitor begins to discharge its stored power across the resistor until it has been fully discharged. Thus neuron is represented as a capacitor ,resistor connected in parallel with a battery (Carlson, 2005)

Then the interface of neurons and the electrodes is considered. To assist the design of the nanofin device, two simplified equivalent electric circuit models are considered. Each model represents one way to get signal from inside of a neuron. In the first option as shown in Figure 3.1, small nanopillars penetrate the cell membrane. In this model, the nanopillar or at least the tip of the nanopillar is electrically in “direct” contact with cytosol (or intracellular fluid). The signal

can pass the interfacial impedance (C_{DL} and R_{ct}) and pillar resistance (R_E) to instrument, or bypass this path through the gap between cell and device (through R_{seal}). Current penetrating device design such as VNEA often has a small cross section area like a thin needle which is best for penetration. Small cross section electrode, having very large interfacial impedance (C_{DL} and R_{ct}) and pillar resistance (R_E), reduces total amplitude of the passing signal and forces current leakage through R_{seal} . In the second option as shown in Figure 3.2, large nanopillar does not really penetrate the cell. The cell membrane still preserves some degree of function, which results in no “direct” electrode-cytosol contact. However, some special shape or coating can make the contacting membrane electrically porous and tremendously reduce the trans-membrane impedance so that the intracellular signal can pass through the reduced trans-membrane impedance, interfacial impedance, and electrode resistance. In this design, we need to minimize not only the by-pass current but also the trans-membrane impedance.

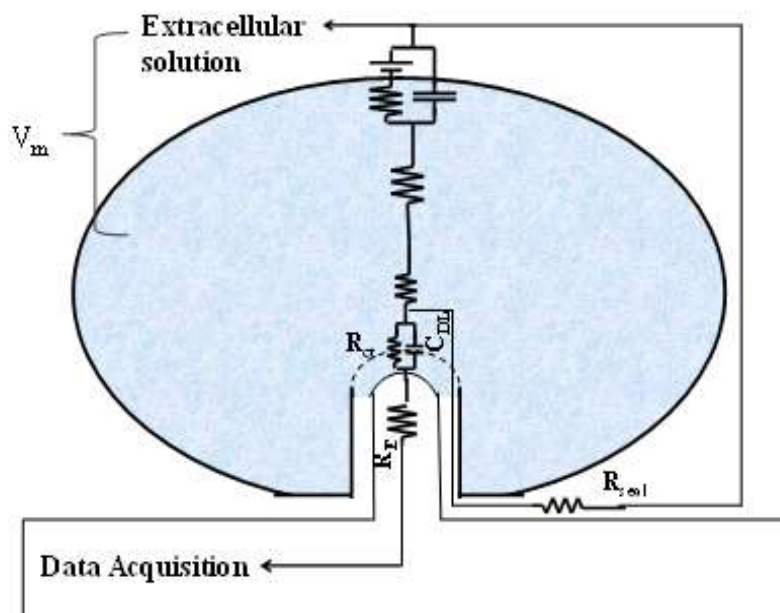


Figure 3.1. Equivalent circuit showing electrode cytosol contact.

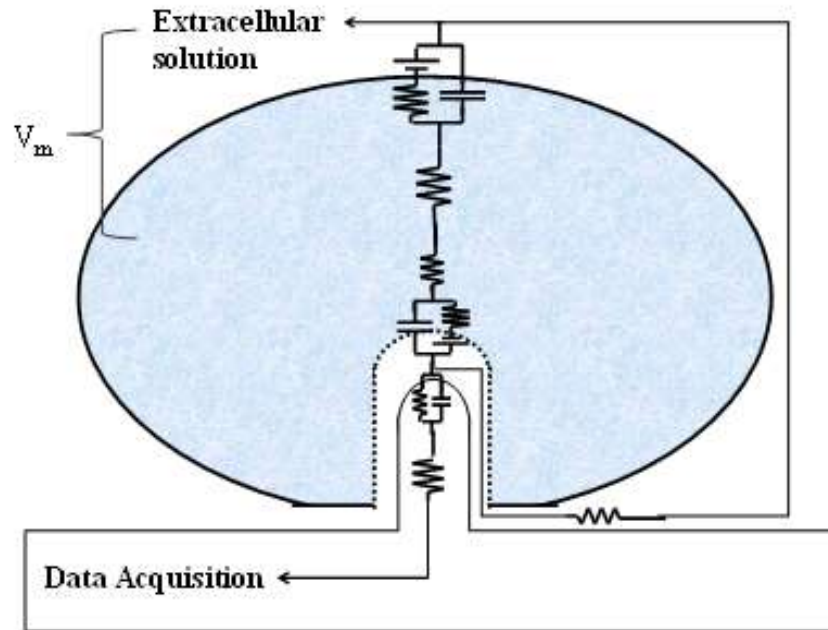


Figure 3.2. Equivalent circuit showing no electrode cytosol contact.

The design of nanofin device is to aim for larger surface area and cross section area of the intracellular electrode that result in the smaller interfacial impedance and electrode resistance. The Figure 3.14 shows a single nanopillar and a nanofin with their dimensions. To calculate the benefit of the fin design, it was assumed that the top one third of the pillar and four fifth of the nanofin are metalized, which provides the electrode surfaces. While 3x3 pillar array or 3x1 nanofin array were used (pitch = 2 μm in both cases), the total metalized pillar surface equals to be 1.4 μm^2 and total metalized nanofin surface equals to be 58.5 μm^2 . The electrode surface increase results in 42 times larger capacitance, one 42th smaller charge transfer resistance. Similar calculation results shows total metalized pillar base area to be 0.07 μm^2 and total metalized nanofin base area to be 1.44 μm^2 ; in such a design, device had one-twentieth electrode resistance as pillars.

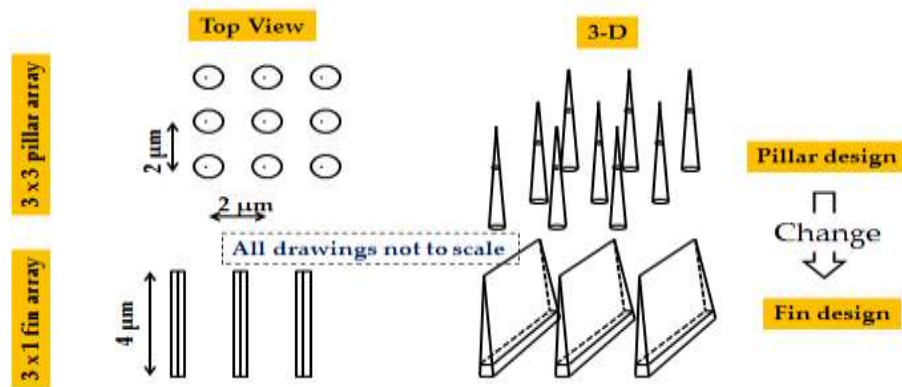


Figure 3.3. Shows conventional nanopillar design to nanofin.

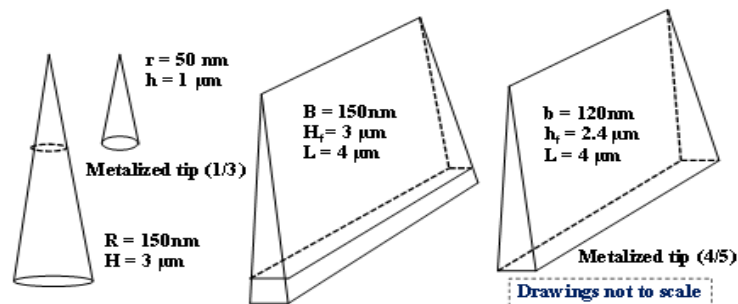


Figure 3.4. Comparison of dimensions of nanopillars with nanofins.

3.2 Fabrication of the Device

3.2.1 Optimization of the FIB process. The main challenge for the intracellular recording is to optimize the nanofin number which reduces the impedance, at the same time finding the appropriate density for internalization (Hai et al., 2010).

Robinson et al have shown that, out of the nanopillars, only a fraction of them penetrate spontaneously and the impedance is too high to record the intracellular potentials (Robinson et al., 2012). Theoretically, increasing the electrode density reduces the impedance but penetration becomes difficult as the high density electrodes behave like a bed of nail. The recordings from Bruggerman et al concludes that high density pillars maintained extracellular position (Brüggemann et al., 2011).

The nanofins were optimized according to the size of the cells. Since the PC 12 cells that are differentiated can reach varied sizes ranging from $1\mu\text{m}$ to $20\mu\text{m}$, two different configurations were considered. First - Large density nanofins were milled. The advantage of this method is less impedance but internalization might be the trade-off. Second - Lesser density nanofins were cut. Here the internalization will be easy and the nanofin design can enable long term recording.

3.2.2 Optimization to find clear cut lines. The first step in the FIB process was to find the ability of each beam to focus properly to a smaller diameter. For the current values of 50pA , 275pA the beam was focused so that 40nm to 60nm trenches can be written.

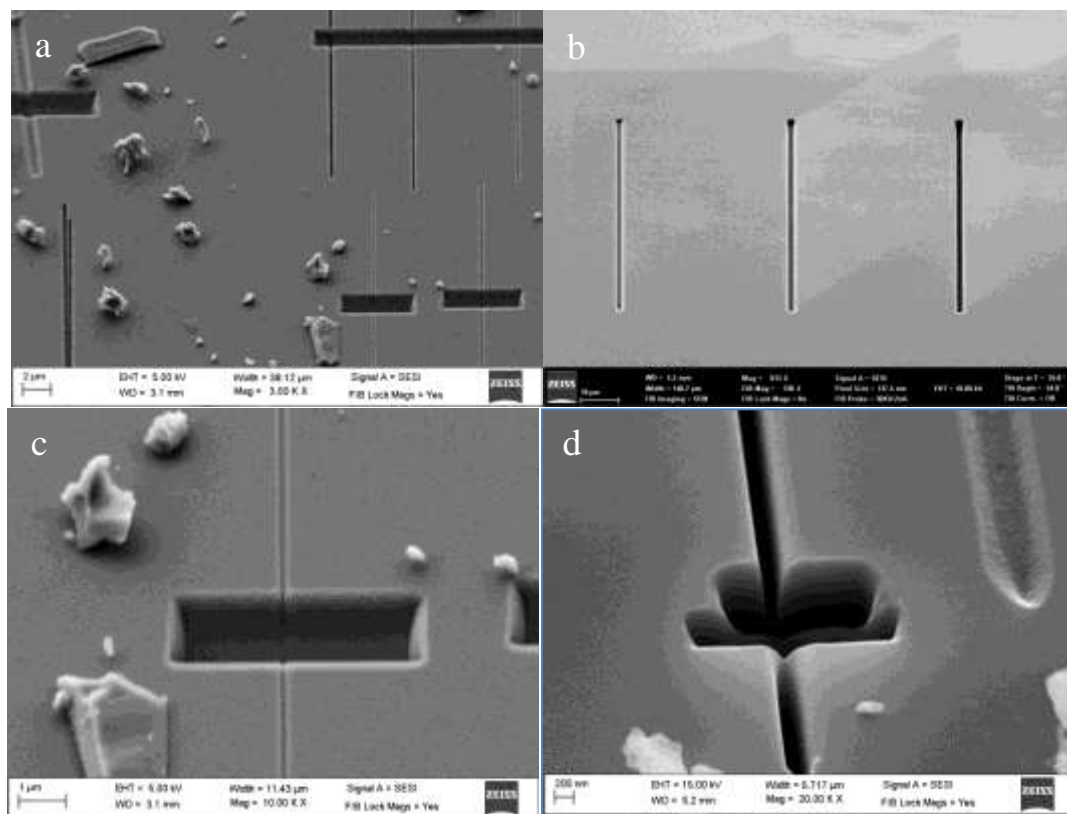


Figure 3.5. Optimization to find clear cut lines: a) Lines in various currents and dosages; b) 2 nA current with 5nC, 10nC and 15 nC dosage from left to right; c) Observation of depth of a vertical line; d) Milling to find the width of the vertical line.

Vertical lines were drawn in various dosages and currents to find whether clear cut lines can be drawn as shown in Figure 3.5 (a and b). Then a larger rectangular cut was milled and observation which gave enough information of the actual depth of each cut was done as shown from the Figure 3.5 (c and d). It can be inferred that lines up to 200nm width can be drawn. The specifications were W 200nm H 50 μ m D 1nC.

3.2.3 Optimization to find the pitch – drawing parallel vertical and horizontal lines.

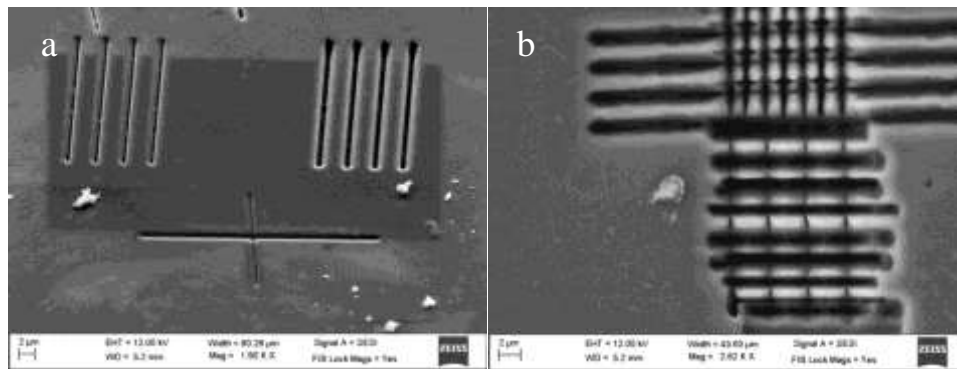


Figure 3.6. Optimization of pitch: a) Parallel vertical lines; b) Parallel horizontal lines and vertical lines.

After finding the current and dosage for clear cut lines, the next step was to find the appropriate Pitch value. Pitch is the distance between the centers of two parallel lines. For this, optimized pitch value, if over the horizontal lines, vertical lines were drawn, then nanofins can be fabricated as shown in Figure 3.6 b.

3.2.4 Effect of dosage and current on milling distance.

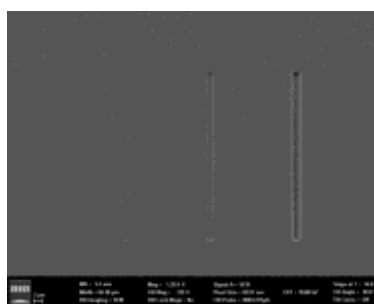


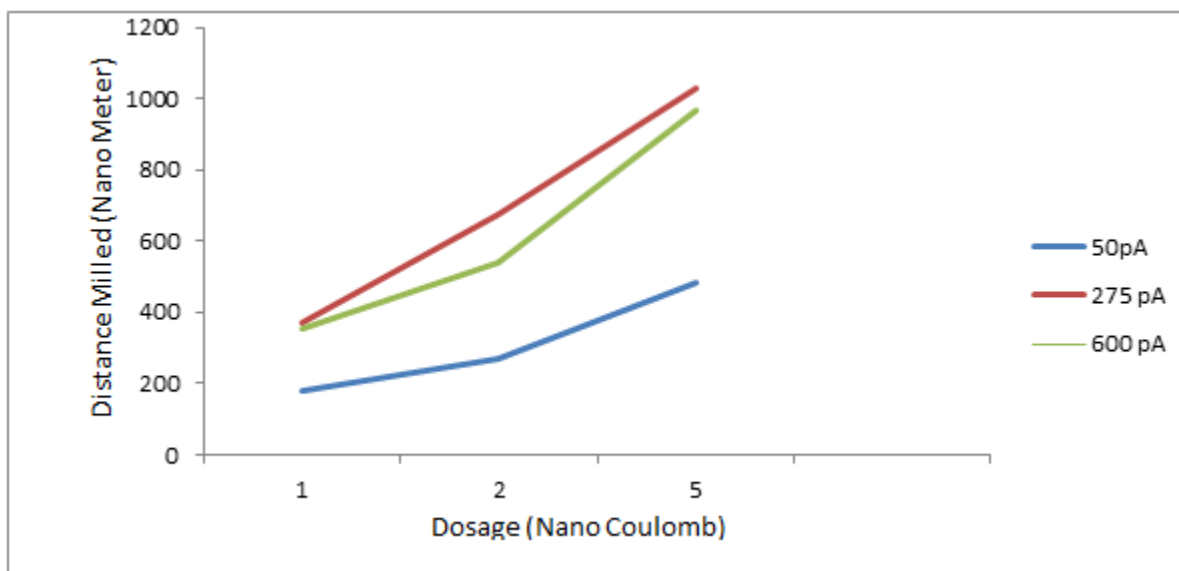
Figure 3.7. Milled lines to show different depths in different dosages.

In order to find the relationship between Dosage and milling distance, for a constant current value, milling was done in different dosages. First, for the current value 275pA, lines were milled with 1nC, 2nC and 5nC dosage as shown in the Figure 3.7. Here the time taken for milling was also noted.

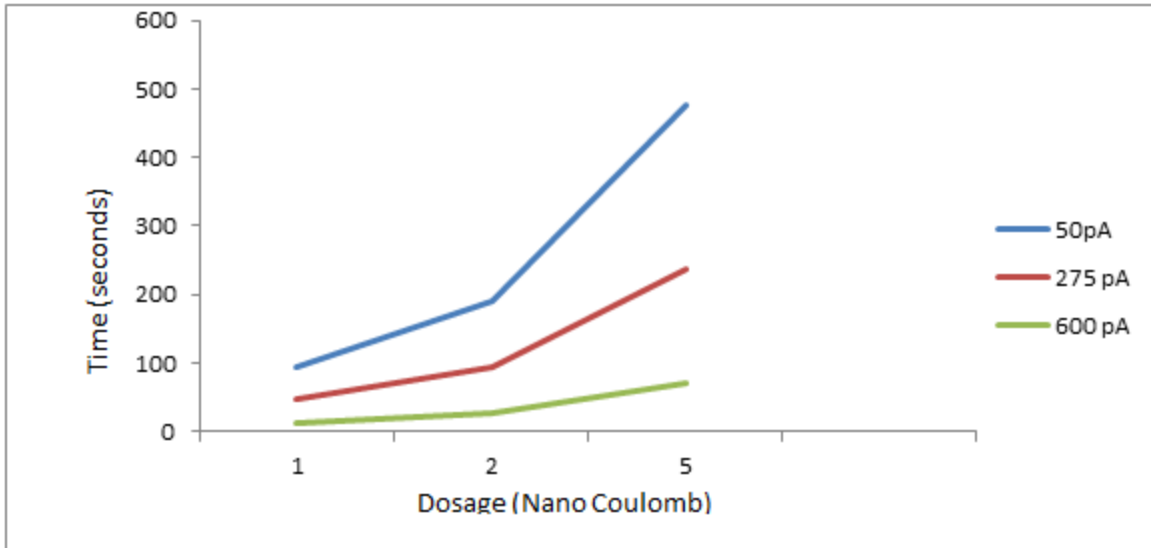


Figure 3.8. Milling done on different dosages: a) 1nC; b) 2nC; c) 5nC.

Then for each dosage lines, rectangular cut was milled to see the depth of milling as shown in the Figure 3.8. Then two graphs were plotted: a) Dosage vs Distance milled and b) Dosage Vs Time



a) Dosage vs Distance milled



b) Dosage vs Time

Figure 3.9. Effect of dosage on milling distance and time: a) Dosage vs Distance milled; b) Dosage vs Time.

From the Figure 3.9 a, it was observed that as the dosage was increased, the milling distance also increased. That is, by increasing the dosage, the height of the nanofin was increased and vice versa. But higher dosage above 10 nC did not yield smaller width lines as the pitch cannot be maintained. Also, the current has to be decreased to mill smaller width lines. Lesser the current value, smaller the aperture is and so is the smaller milling distance. So in order to get the nanofin size up to 200 nm the optimized current was 275 pA. From the figure 3.9 b), it can be shown that as the dosage was increased, time to mill also increased. Considering the time factor, reducing the current to 50 pA can give still smaller width pillars up to 100 nm but the milling time will be very high.

3.2.5 FIB first SOI process flow. Three different process flows were considered for the fabrication. In the first method, the steps are milling of nanofins on the Silicon over Insulator (SOI) wafer, oxidation of wafer, gold (Au) deposition using Physical Vapor Deposition (PVD)

and finally Au patterning. The main advantage of this method is that the signal will leak from the Au surface not covered by cells. So, this process flow was skipped and the other two process flows were implemented.

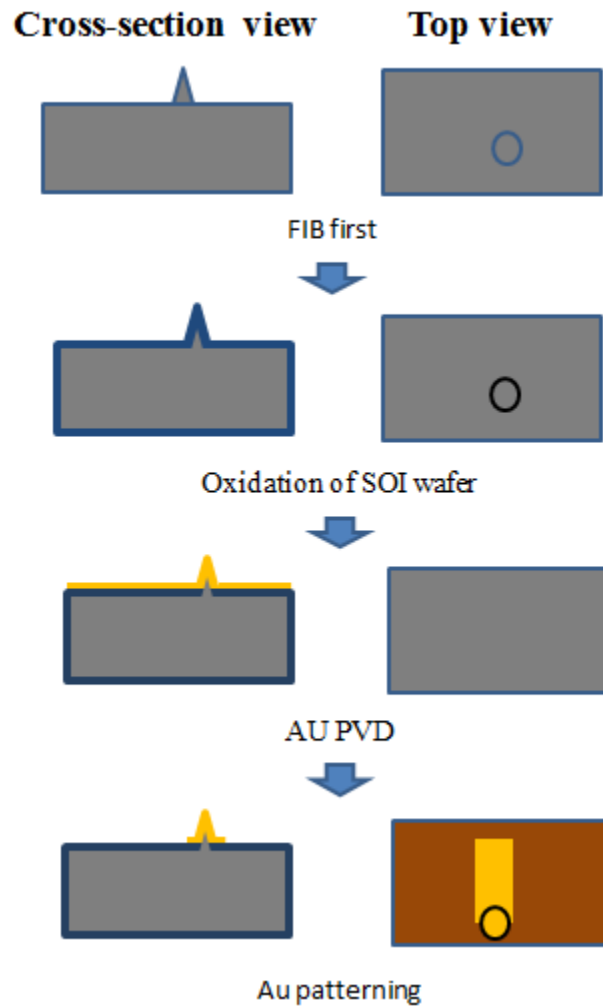


Figure 3.10. Schematic representation of FIB first SOI based design.

3.2.6 EBL process flow. In the second process flow, the fabrication starts with silicon substrate. First, the nanofins are milled over specific micrometer sized area. Then oxidation is done to insulate the whole wafer. Au PVD covered the insulated wafer. Lithography and Au wet etch defines the gold nanofin connection lines, and contact pads. Then a thin coating of photosensitive polymer, PMMA (Poly methyl methacrylate) is spun over to cover the whole

wafer. Electron beam Lithography (EBL) etches the polymer in the nanofin areas and contact pads. In this configuration, the nanofins are the Au Fins. The insulating layer is the polymer layer.

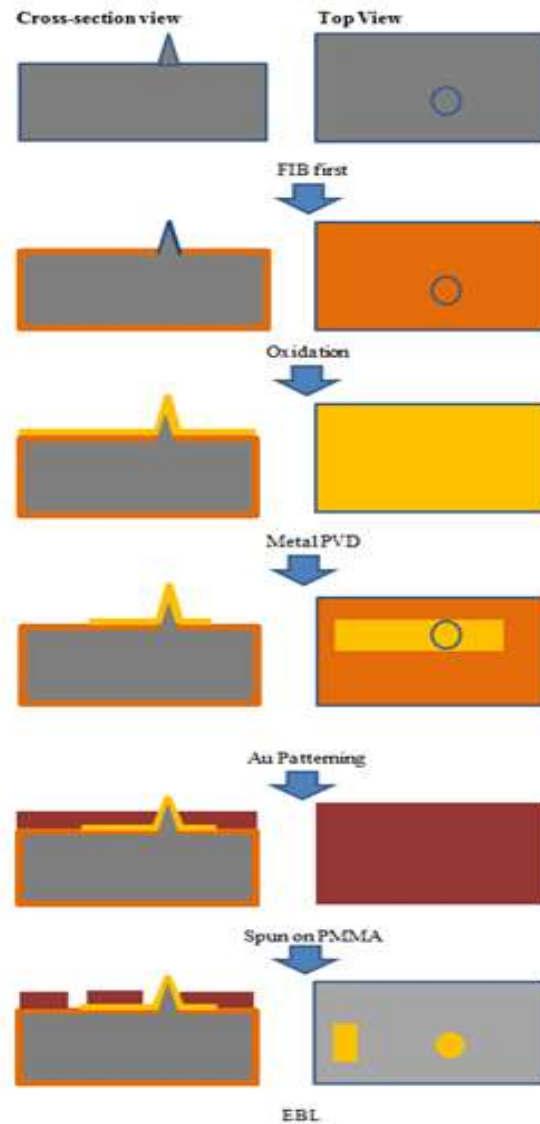


Figure 3.11. Schematic representation of EBL process flow.

For this process flow, the first step was to mill high density nanofins on a silicon substrate. Silicon wafers were purchased from Wacker Siltronic (Item # PB1194). For milling, optimization was done by aligning in a straight line both horizontally as well as vertically.

3.2.6.1 Optimization of high density nanofins. First parallel vertical lines were drawn and then followed by parallel horizontal lines. This approach had an alignment issue where each horizontal line was shifted to the left by a certain distance as shown in the Figure 3.12.

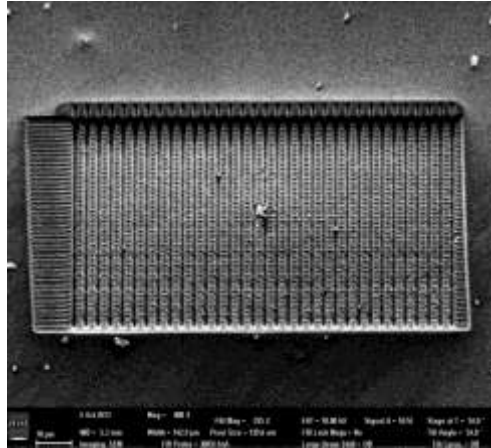


Figure 3.12. Horizontal lines shifting to the left.

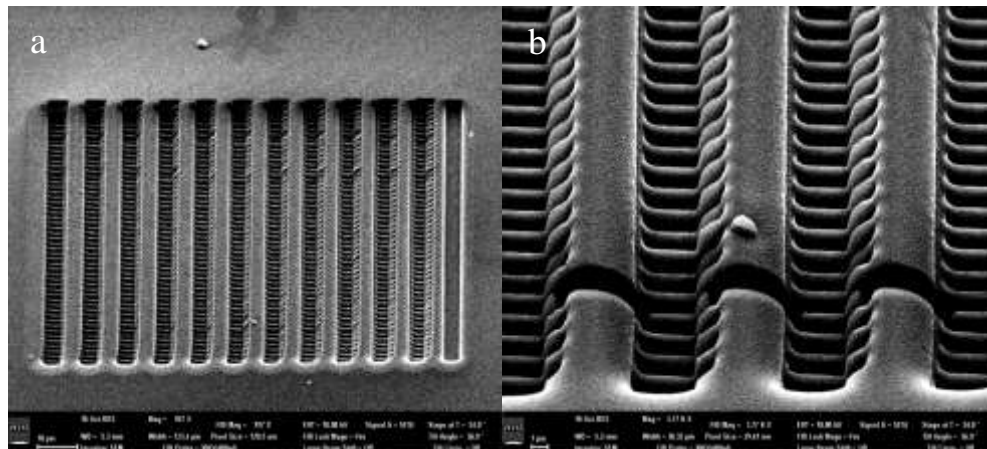


Figure 3.13. Position of the cut: a) Milling done in trough instead of the crest; b) Deeper ridge was cut to observe the details.

Also, there was misalignment with respect to the position of the second cut which made the whole cut shift by one position of the slot, in consequence milling was done in the trough region instead of the crest region as shown in the figure 3.13. After troubleshooting the beam

alignment in the Auriga SEM and switching the strategy from drawing the horizontal lines first, the misalignment issue was resolved.

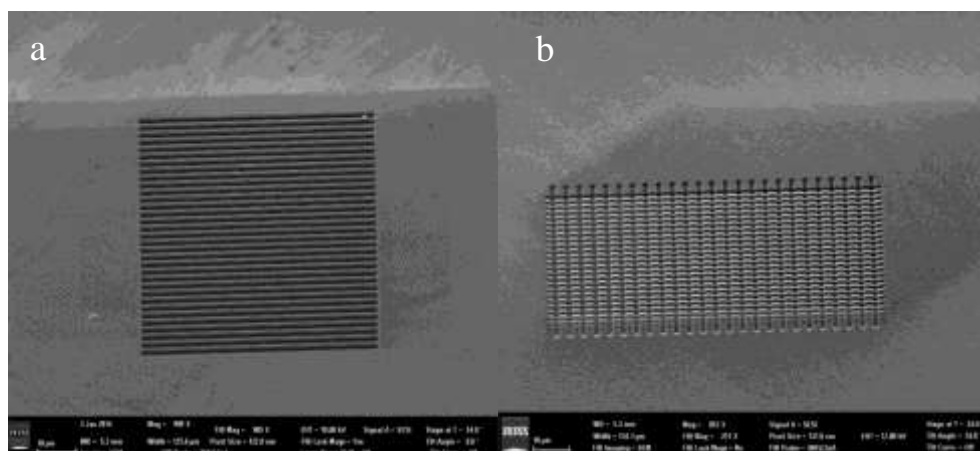


Figure 3.14. High density nanofins: a) Aligned horizontal lines; b) Nanofin structure.

First, 34 horizontal lines were drawn as shown in the Figure 3.14 a). Then, over the aligned horizontal lines, vertical lines were drawn to give nanofin structure. The maximum width possible for high density nanofins was in the range 400 to 600 nm.

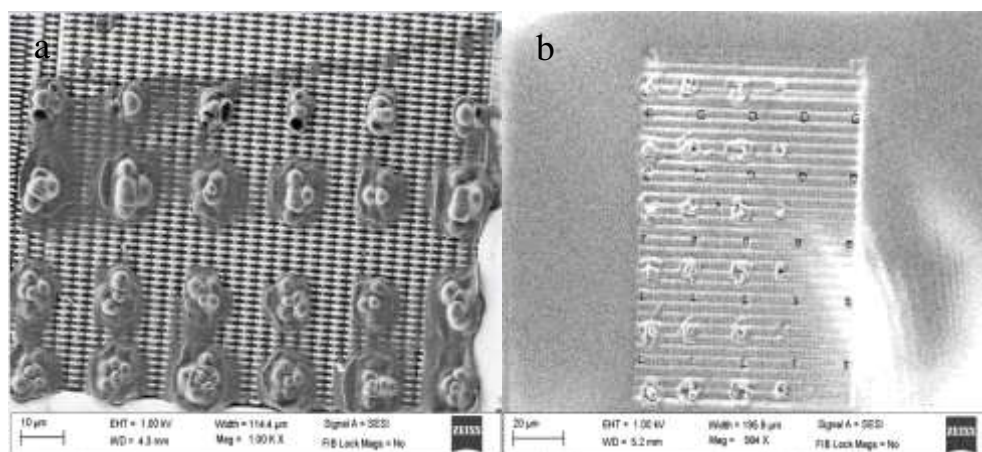


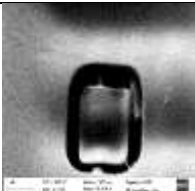
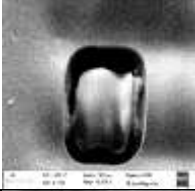
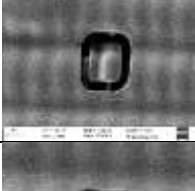
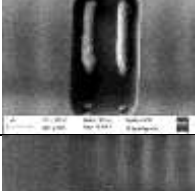
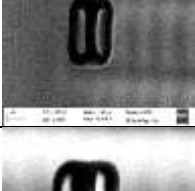

Figure 3.15. Nanofins after electron beam lithography: a) Bubbles showing the hardened region; b) Squared region showing the nanofins.

The next step was the deposition of 50 nm thick gold by PVD over the substrate. Then, over the nanofins, PMMA was spun and then e-beam lithography was done. But in the initial

stage the exposed region became hardened instead of being etched away as shown in the Figure 3.15 a). Then, the beam intensity was reduced and then exposure and further development using methyl iso butyl ketone (MIBK) and iso propyl alcohol (IPA) gave good results and the region shown to e-beam got removed as shown in Figure 3.15 b). The optimum beam condition to get the complete etching away of the polymer was found by trying different dosages.

Table 3.1.

Optimization of e-beam dosage.

Number	Spacing	Dosage	Specification	SEM image
5	20 μm	1 nC	2 \times 2 μm squares	
2	20 μm	2 nC	2 \times 2 μm squares	
1	20 μm	5 nC	2 \times 2 μm squares	
3	20 μm	0.5 nC	3 2 \times 2 μm squares	
1	20 μm	0.2 nC	1 2 \times 2 μm squares	
5	20 μm	0.1 nC	5 2 \times 2 μm squares	

From the above table, it can be inferred that 0.2 nC was the optimized value, since the nanofins were completely etched for easier cell contact.

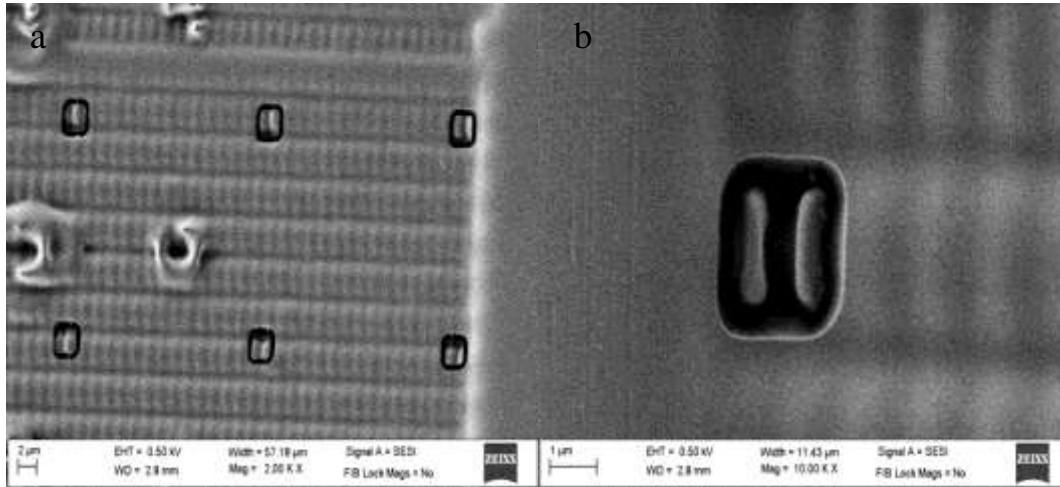


Figure 3.16. Nanofins after dosage optimization: a) Nanofins after showing e-beam; b) Two nanofins with 0.2 nC dosage.

The e-beam shown over the PMMA layer etches the polymer so that nanofins can be shown as in the Figure 3.16.a). The dosage optimization of 0.2nC gave good results, where the polymer was fully etched and the cell contact can be easy as shown in Figure 3.16 b).

The advantage of this method is that it can be very sensitive since the nanofins are sealed and all other region except the nanofin was insulated. But in this method, growing the cells over the nanofins will be a challenge. Further optimization has to be done to make the exposed nanofins taller than PMMA surface so that cells can be easily penetrated. So, further device fabrication using gold wet etch process was not done.

The third SOI based design with Si Conducting lines and contact pads completely insulated by SiO₂ layer and having gold coated nanofins was selected.

3.2.7 SOI based design. In the third SOI based design, oxidation and then BOE process is followed to pattern oxidation. Then Si etching is done to get the device. And then milling is done to fabricate the nanofins as shown in the Figure 3.17.

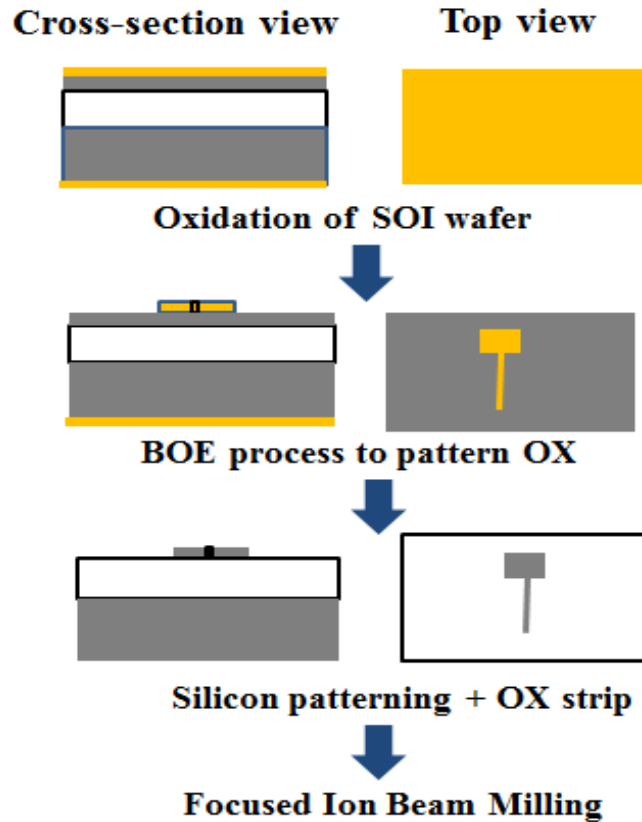


Figure 3.17. Schematic representation of SOI based design.

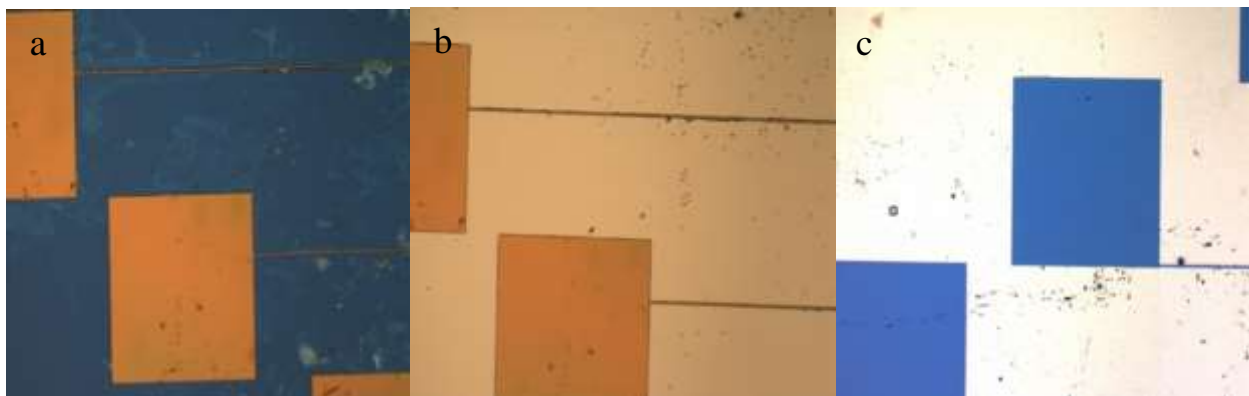


Figure 3.18. Intermediate steps in the SOI process flow: a) After developing by MF-321; b) After oxide etch by BOE; c) After Si etch by KOH.

As shown in the Figure 3.18, the SOI wafer was first oxidized by dry oxidation. SOI wafer was purchased from University Wafer (Item # 912). Oxygen purge was done at 1000 degree C for 3hrs to achieve the targeted oxidation of 100 nm. Then photoresist was coated over the wafer. Thickness of the resist depends on the speed of the spinner. Thickness and exposure time was optimized according to the data sheet. After exposure to ultra violet (UV) light, developing was done by treating with MF-321. Next patterning SiO₂ was done by Buffered oxide etch, BOE (10 : 1) for 3 minutes. After that, silicon etching was done by treating with 15% potassium hydroxide (KOH). Finally FIB was done to fabricate the nanofins.

3.2.7.1 Optimization of low density nanofins. First, the nanofins were optimized in order to get the required number of nanofins by milling directly.

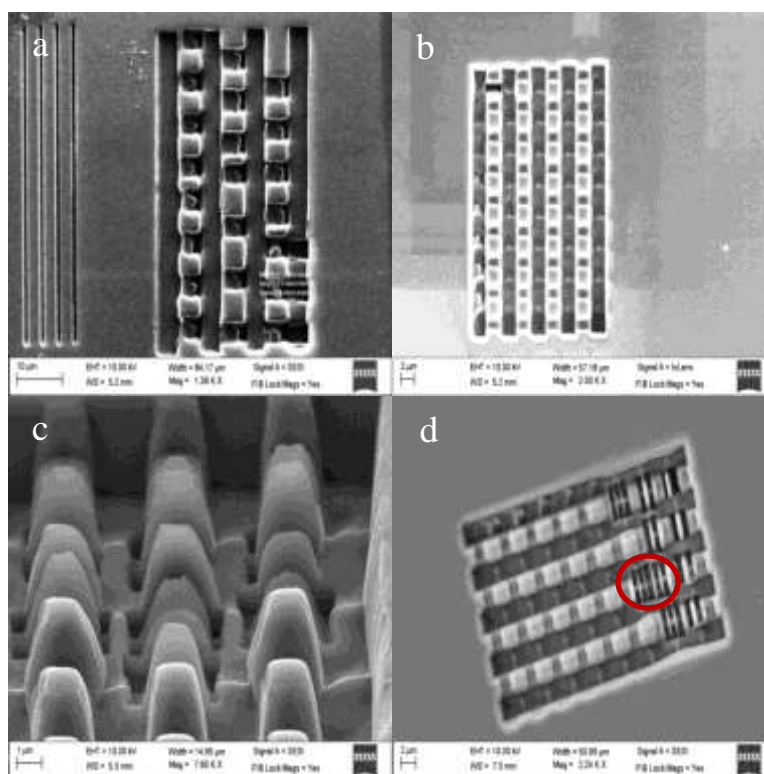


Figure 3.19. Optimization of current: a) Specification for 4 by 4 μm squares; b) 4 by 4 μm squares with 12 nA 10nc; c) Nanofins with various currents and dosages; d) 300 nm nanofins.

To find the optimum values of current and dosages, first a 4*4 μm square area was milled. For the thick vertical lines after trying 12nA, 4 nA and 1nA, 12 nA was chosen because of the clear cut lines as well as the faster FIB time as shown in the Figure 3.19 a) and b). Then to find the optimized values for the nanofins, 1nA, 2 nA, 600 pA, 275 pA and 50pA were selected and nanofins with dosages of 5nc and 10 nc were tried and finally thin nanofins up to 300 nm were milled by 275 pA, 10 nC as shown in the Figure 3.19 c) and d).

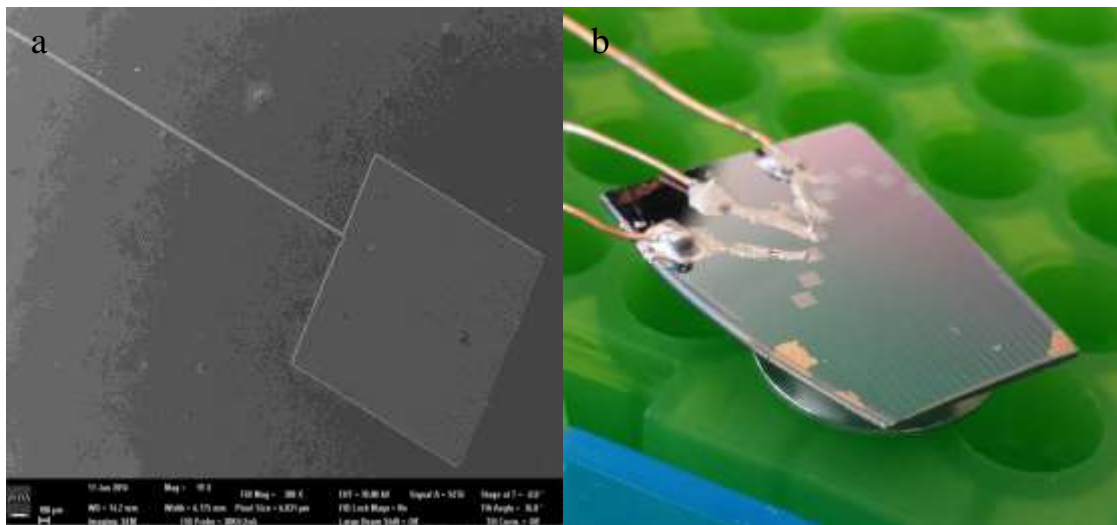


Figure 3.20. Device: a) Contact pad and track lines; b) Device with contact pads and conducting wire.

After finding the optimized value in a silicon wafer, the set of values were again tried in the device. The device consists of contact pads and track lines to make electrical connections as shown in Figure 3.20 a). Output was taken from the contact pads by conducting glue and copper wire as shown in Figure 3.20 b).

3.2.7.2 Optimization up to 200 nm.

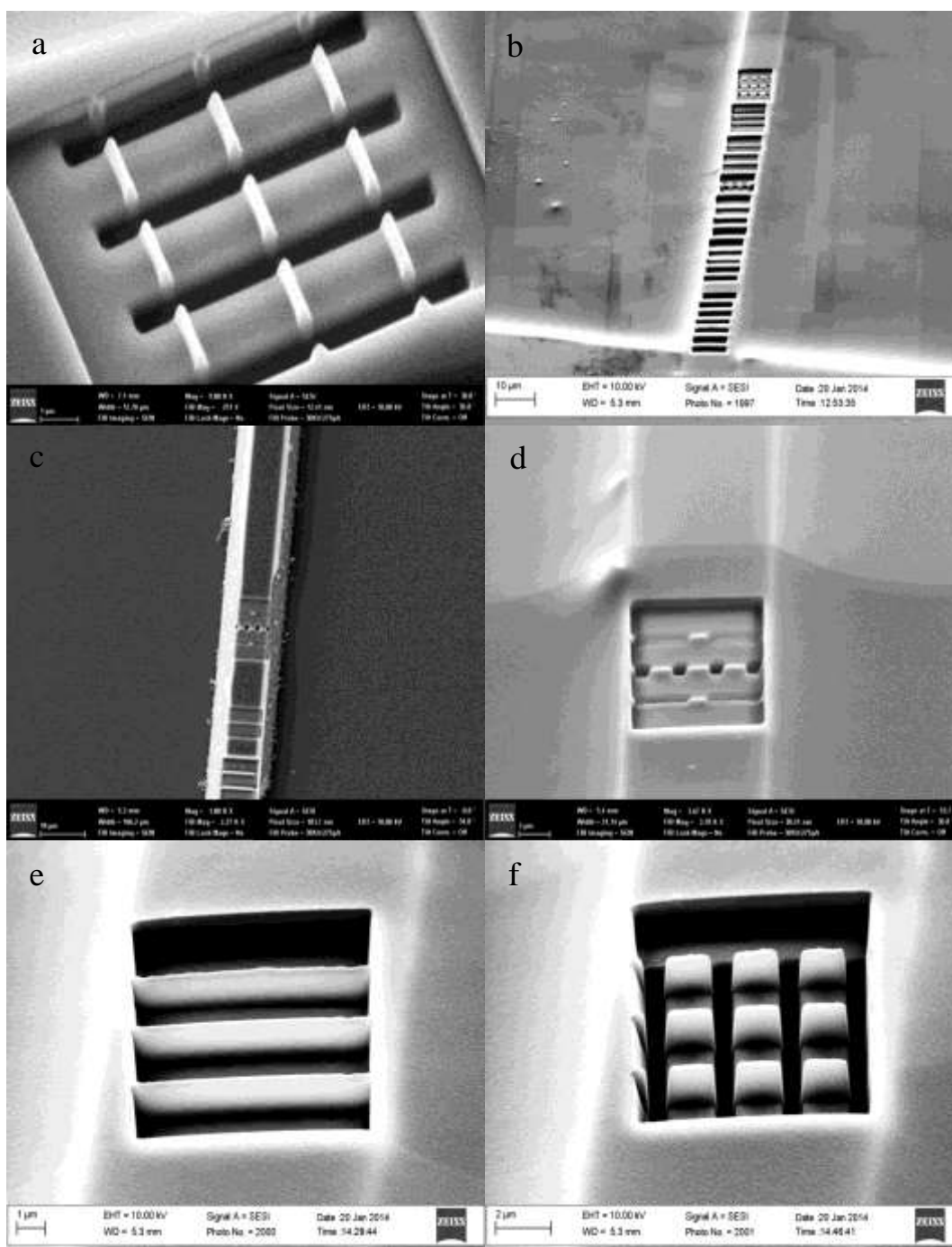


Figure 3.21. Optimization of nanofins up to 200 nm: a) Width optimization; b) 200 nm width nanofins; c) Width optimization; d) 200 nm width nanofins; e) Placement chamber after height optimization; f) 200 nm width, 1 μm height nanofins.

To further optimize the nanofins to lower values, horizontal lines with various heights (H) and widths (W) were drawn. The pitch (S) was adjusted to the possible lowest level to get the minimum width of 200 nm as shown in the Figure 3.21 a),c)and e).And then vertical lines were drawn to get the nanofins as shown in the Figure 3.21 e) and f).Figure 3.21. Shows detailed optimization of various nanofin sizes.

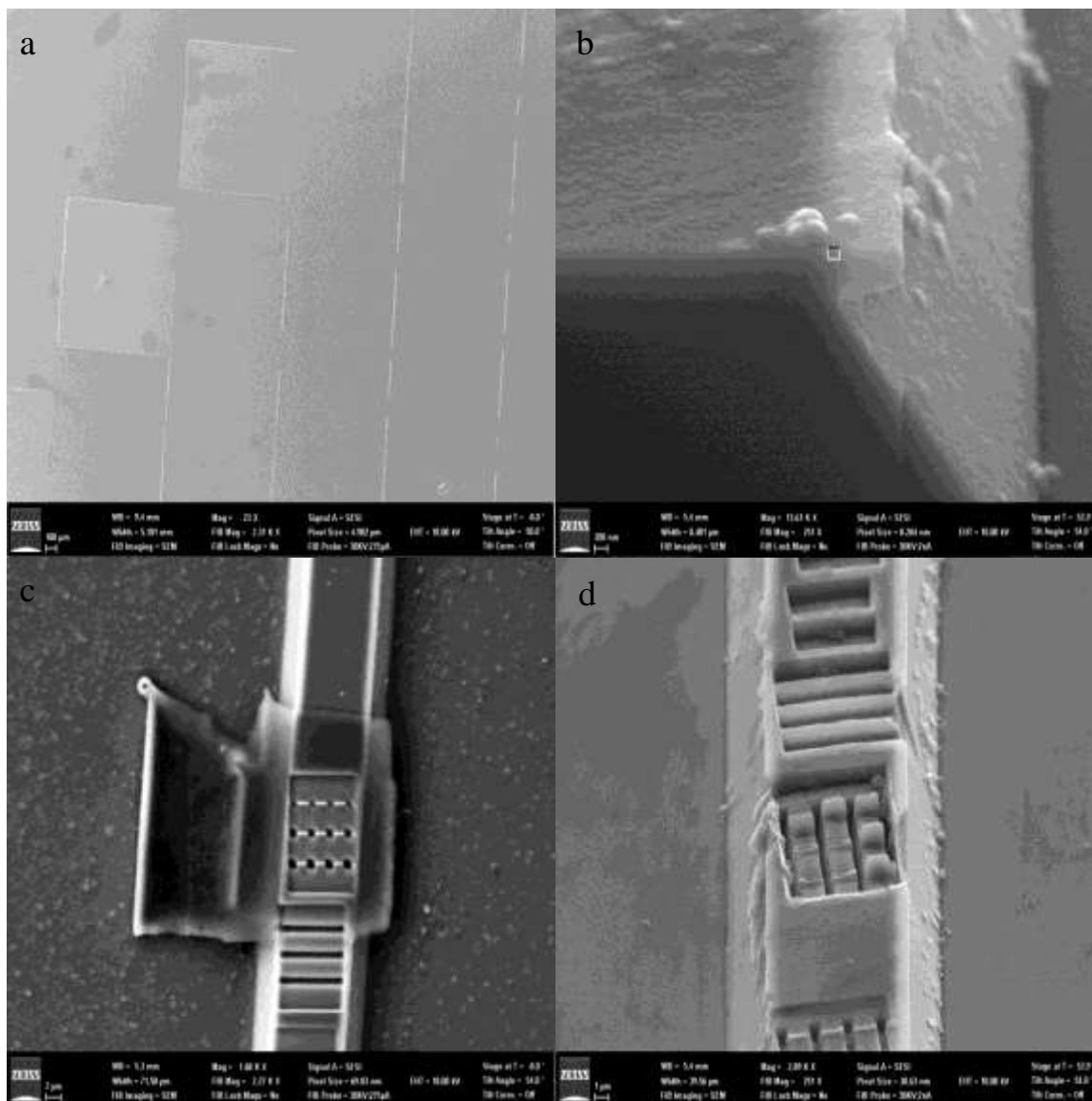


Figure 3.22. Changes during the process flow: a) Open track lines; b) Oxidation details; c) Photoresist not removed with acetone and IPA; d) Fins eroded after treating with piranha.

During the process flow, there were open spaces in the track lines as shown in the Figure 3.23 a) The reason for this may be due to the over exposure of UV light or the inconsistency in the etch time. After reducing the exposure time from 7 seconds to 5 seconds, the problem was resolved. In the process flow, the lift off using PR was first decided. But the ion beam made the PR hardened and it was difficult to remove with acetone and IPA as shown in the Figure 3.23 c). Further treatment with piranha eroded the nanofins as shown in the Figure 3.23 d).

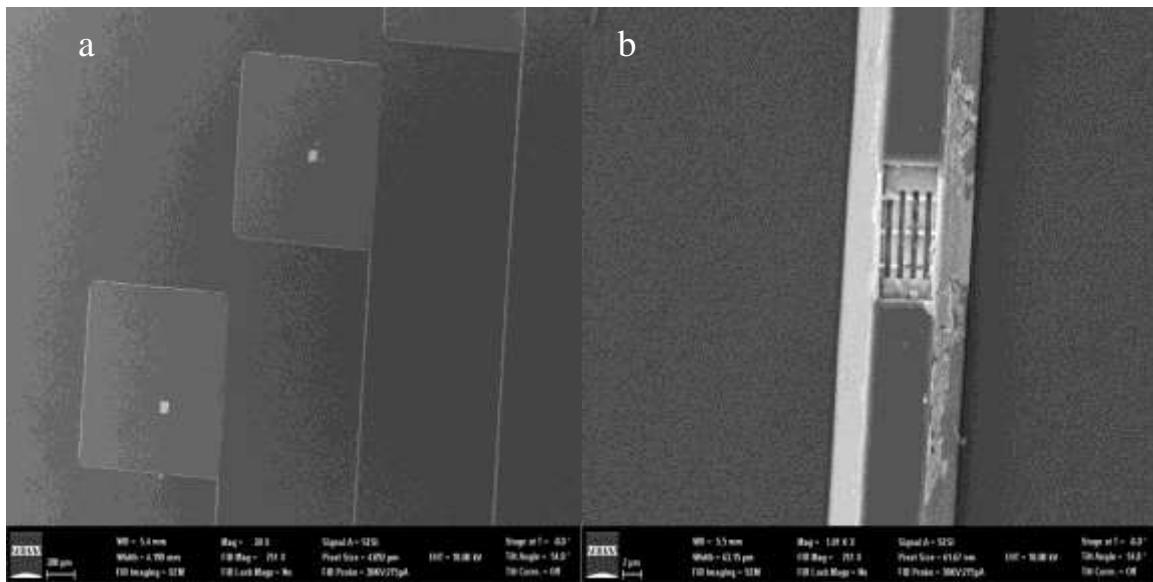


Figure 3.23. Gold coating over the milled region: a) Gold in the milled area of the contact pad; b) Gold over the nanofins.

So, Aluminum (Al) lift off was decided and Al was coated using thermal evaporation. And then milling was done. And then gold was deposited. Al Lift off was done so gold remains in the milled area i.e. over the nanofins and the milled portion of the contact pad as shown in the Figure 3.24 a),b).

Table 3.2.

Nanofin structure in five of the track lines over the device.

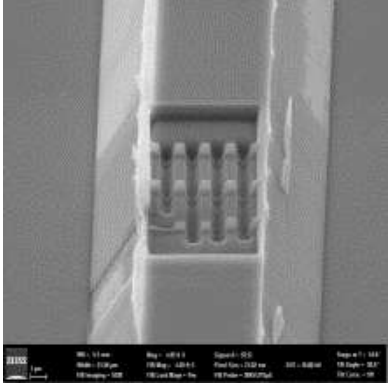
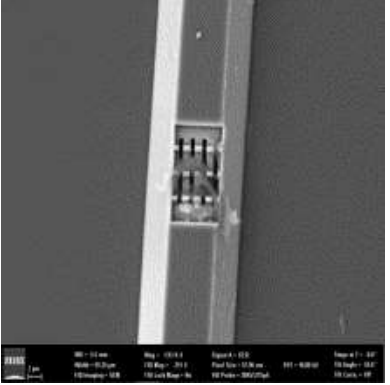
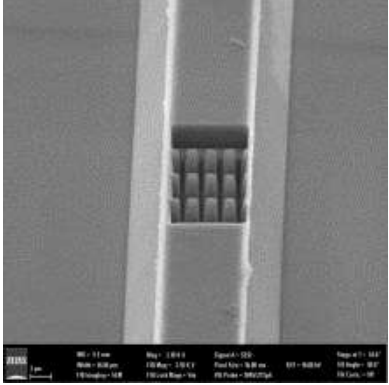
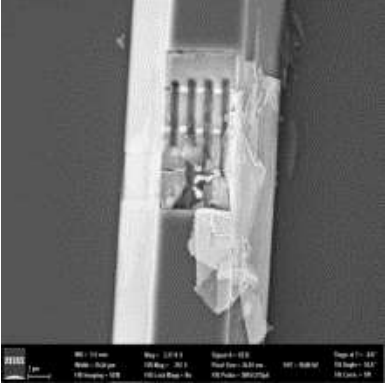
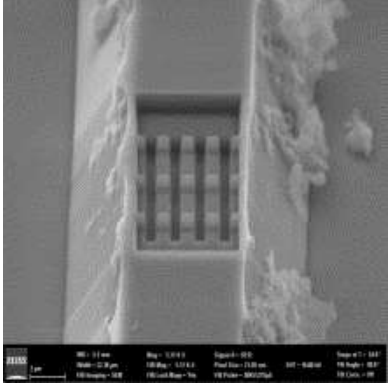
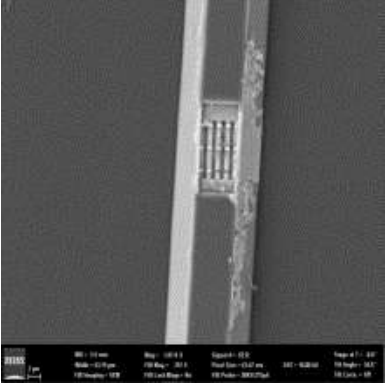
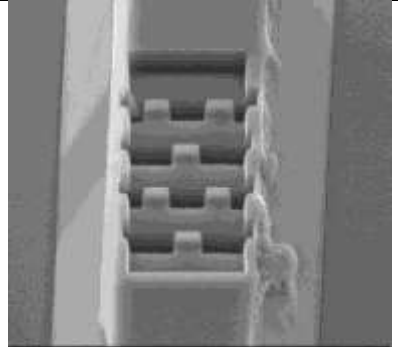
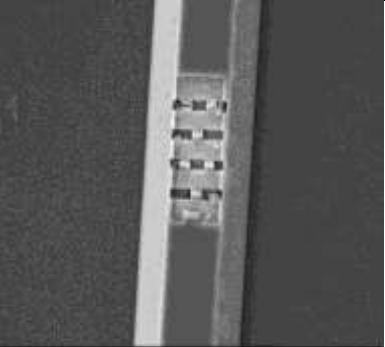
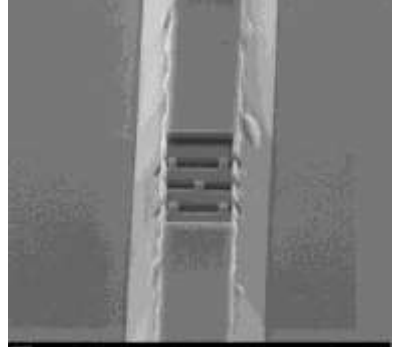
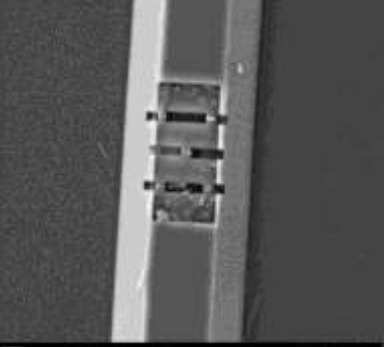
Nanofins after Al coating	Nanofins after gold deposition and Al lift off	Dosage	Height(H)	Width(W)	Pitch(S)
		6	3	6	3.3
		5	3	6	3.3
		6	3	6	3.3

Table 3.2.

Cont.

 <p>SEM image showing a series of nanofins on a track line. The image shows a cross-section of the device with several horizontal bars (nanofins) extending from a central track line. The bars are separated by small gaps. The track line is flanked by vertical structures.</p>	 <p>SEM image showing a series of nanofins on a track line. The image shows a cross-section of the device with several horizontal bars (nanofins) extending from a central track line. The bars are separated by small gaps. The track line is flanked by vertical structures.</p>	6	3	6	3.3
 <p>SEM image showing a series of nanofins on a track line. The image shows a cross-section of the device with several horizontal bars (nanofins) extending from a central track line. The bars are separated by small gaps. The track line is flanked by vertical structures.</p>	 <p>SEM image showing a series of nanofins on a track line. The image shows a cross-section of the device with several horizontal bars (nanofins) extending from a central track line. The bars are separated by small gaps. The track line is flanked by vertical structures.</p>	6	3	6	3.2

A device was fabricated with conducting Si tracks insulated by silicon di oxide layer for good conductivity and signal strength. 200 nm nanofins were fabricated over the track lines. The next step was to culture cells over the nanofins.

CHAPTER 4

Growing Cells over Nanofins

In this chapter, optimization of cell culturing, adherence and differentiation protocols for cell nanofin interface is explained in detail.

The steps were,

- a) Optimization of adherence protocol of PC12 cells over Au nanofins.
- b) Cell culturing over nanofins.
- c) Differentiation of PC 12 cells into neurons.

4.1 Cell Lines

PC12 cells are a cell line derived from the pheochromocytoma – a neuroendocrine tumor – of the rat adrenal medulla. These cells are isolated by Greene and Tischler and are a useful model for studying neuronal properties.

The PC12 cells are adrenal chromaffin-like cells which are capable of differentiating into a more neuronal phenotype using e.g., NGF, or into a more neuroendocrine endothelial cell-type using glucocorticoids like dexamethasone. The former cell line has been used as paraneurons. Paraneurons are those cells which have not been designated as neurons but are recognized as closely related to neurons on the basis of their fine structure (possession of neurosecretion-like and synaptic vesicle-like granules/vacuoles), metabolism (production of neurosecretion- and neurotransmitter-like substances) and origin (evidenced or proposed neuroectodermal)” (Fujita, 1976).

A neuron-like characteristic is achieved by stimulating the cells with nerve growth factor (NGF), the standard neurotropic substance. In both the cases, the cells synthesize and store catechol amines (dopamine and sometimes norepinephrine), and then released through

exocytosis (Tischler et al., 1986). Several recent studies have demonstrated that these cells display excitable mechanisms whose expression is influenced by nerve growth factor (NGF) and they exhibit a number of properties that resemble rather closely those of sympathetic neurons. This makes PC12 cells useful as a model system for neuronal differentiation and hence forth the action potential measurement. PC12 cells can generate an action potential after treatment with nerve growth factor (Mandel, Cooperman, Maue, Goodman, & Brehm, 1988).

The PC-12 cells were obtained from ATCC (Item # CRL-1721) and cultured in RPMI media which consists of 10% horse serum, 5% fetal bovine serum, and 1% penicillin .The cells were cultured in 75 cm² cell culture flasks at 37 ° C. Media was changed once in two days and passaging of the cells was done once a week to allow healthy growing conditions.

A549 cells are adenocarcinomic human alveolar basal (lung) epithelial cells.A549 cells were obtained from ATCC (Item # CCL-185) and cultured in F12-K media supplemented with 10% fetal bovine serum and 1% penicillin/streptomycin. Cells were fed every two-three days and sub cultured every 5 days to allow healthy growing conditions.

4.2 Optimization of Adherence Protocol of PC12 Cells over Au Nanofins

The main goal was to find the biocompatible material for the adhesion of PC12 cells. In this regards, Poly-Ethylene-Imine (PEI), Poly-Ethylene-Glycol (PEG), Poly -D-Lysine (PDL) and collagen were considered.

4.2.1 Adherence by physisorption. Initially, collagen was the choice due to biocompatibility as well as the ease of adherence by physisorption. Here the adherence principle is the electrostatic interaction between the cell and the coated surface .Here the molecule is held together by means of weak polarization interaction.

4.2.1.1 Experiments with collagen. Collagen was purchased from Corning (Item # 54254). Over the silicon substrate with nanofins, collagen was coated for adherence and PC 12 cells were cultured and observed under Auriga SEM and following images were obtained.

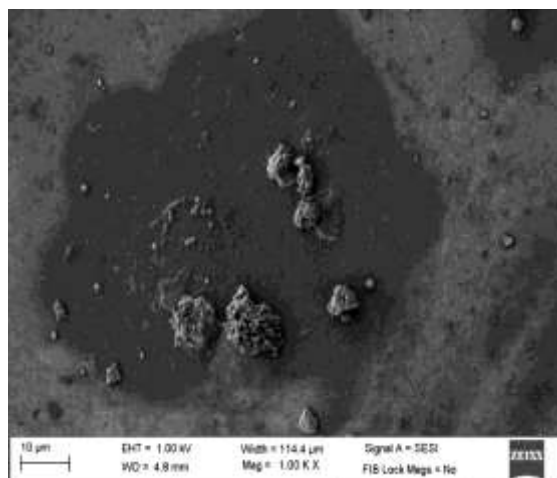


Figure 4.1. PC 12 cells adhered over the collagen coated Si substrate.

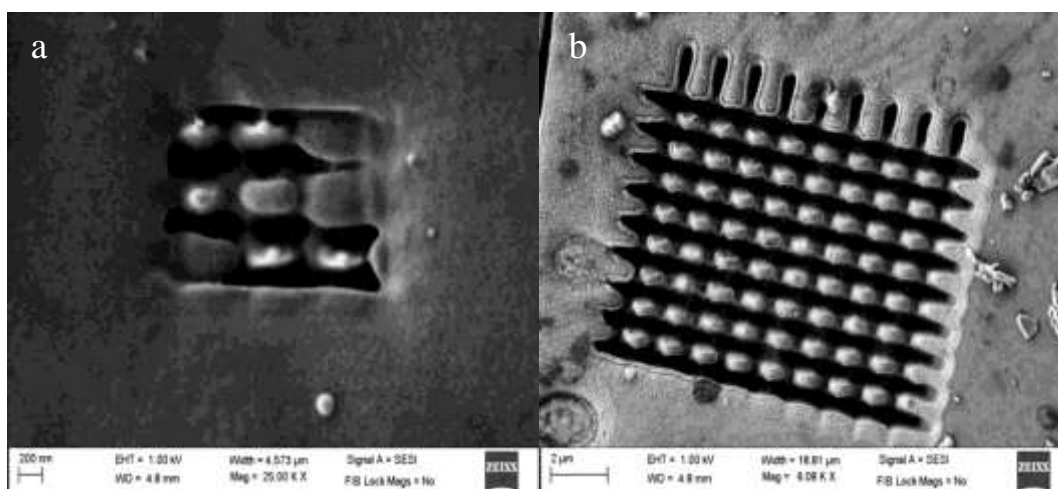


Figure 4.2. Collagen covering the nanofins.

Collagen covered the nanofins uniformly but there were no PC12 cells over the nanofins as shown in Figure 4.2. Placing the cells over nanofins was challenging.

4.2.2 Adherence by physisorption and chemisorption. The goal was to immobilize the cells on the gold nanofins. Since gold surface was used, collagen was not favorable for

immobilization. PDL was the better choice since functionalization of gold can be easily done by covalent cross linking by amide bonding.

In chemisorption, the molecules are held together by means of sharing of electrons by covalent bonding (Lennard-Jones, 1932). Cell adherence is strong and they can remain attached for longer duration.

4.2.2.1 SAM formation. Self-Assembled Monolayers (SAMs) are molecular assemblies in order, which are formed spontaneously. The common protocol to produce SAMs is to put cleaned substrates in diluted ethanol solution of the thiols for 18 to 24 hours. Here simple Langmuir growth takes place proportional to the available active sites (Love, Estroff, Kriebel, Nuzzo, & Whitesides, 2005). Factors that influence SAM formation are the solvent, the cleanliness of the substrates, and concentration of the solution. Ethanol is one of the common solvent used for alkane thiols in the SAM formation step. Cleanliness of the substrates is important because the impurities delay the SAM formation. The concentration of the solution relates to the immersion time. Typically concentration in the range of mM is used (Schreiber, 2000).

4.2.2.2 Cross linking. Carboxylates can react to NHS (N-hydroxy succinimide) in the presence of EDC (1-ethyl-3-(3-dimethylaminopropyl)carbodiimide) to form a semi stable NHS ester which reacts with amine groups to form amide bonds. Also, gold functionalization can be done by Thiol SAM formation, crosslinking by EDC NHS and final treatment with PDL (Nam, Chang, Wheeler, & Brewer, 2004). Also, PDL may weakly bind to gold anyway because there is some affinity between NH₂ groups and gold.

4.2.2.3 Experiments with PDL. First the substrates were treated with lipoic acid for 24 hours in order to get the SAM layer and then treated with PDL for cell adherence. PDL was

purchased from Corning (Item # 354210). Gold coated wafers were taken and washed with acetone for 5 minutes, with ethanol for 2 minutes, and IPA for 2 minutes. Then the wafers were treated in plasma cleaner for 10 minutes.

A six well plate was taken and the following conditions were examined. For the thickness of 20 nm and 120 nm coating of gold substrates, combination of lipoic acid, PDL and just PDL alone as the positive control and with glass without any coating as a negative control was taken. After lipoic acid treatment, the six well plates were sealed and kept in the cell culture hood for 24 hours. Then the wafers were washed in alcohol and treated with PDL and kept for 48 hours in the refrigerator at 4 degree then, the samples were washed with deionized water. Cultured PC12 with the viability of 95% were taken. They were centrifuged and 12ml of fresh media was added. In each of the wells in the six well plates, 410,000 cells per ml were added and kept in incubator for 24 hours. After that wafers were transferred to the single well plate and observed under ZEISS Z2M imager using 10X magnification.

When the wafer coated with 120nm gold and treated with lipoic acid and PDL was observed, fewer numbers of cells were formed as clusters and they were non- uniformly distributed and they were healthy as shown in Figure 4.3 a). Then the wafer coated with 20nm gold and treated with lipoic acid and PDL was observed. Larger PC12 cells form clusters and were evenly distributed and they were healthy as shown in Figure 4.3 c). The wafer coated with 120nm gold and PDL alone was observed, large number of PC12 cells form clusters and they were evenly distributed and they were healthy as shown in Figure 4.3 b). The wafer coated with 20nm gold and with PDL alone showed fewer number of PC12 cells as shown in Figure 4.3 d). On the untreated wafer, no cells were adhered. Also on the glass, no cells were adhered. Later,

they were washed with PBS (Phosphate Buffered Saline) and fresh media was added and observed under microscope after 96 hours.

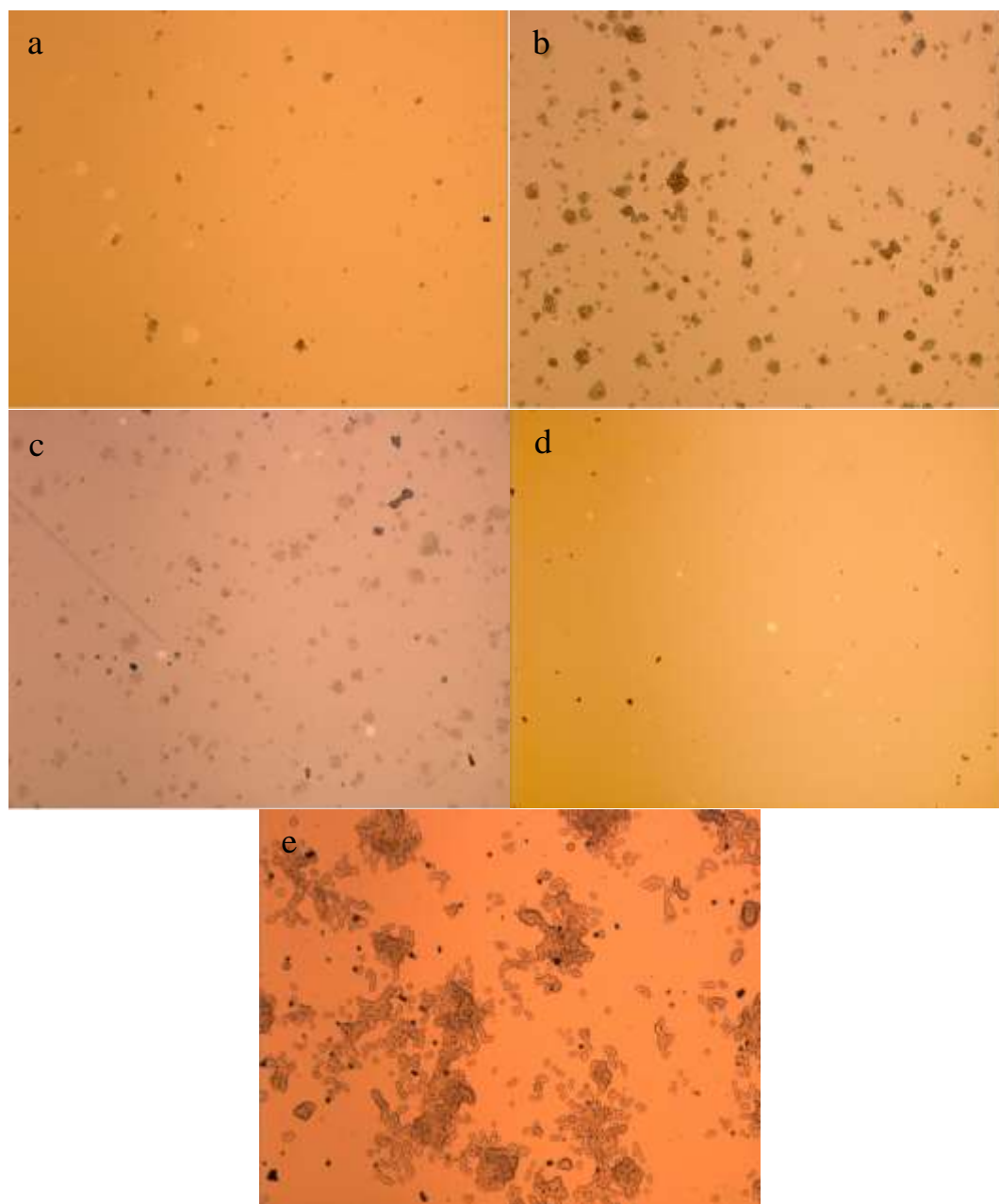


Figure 4.3. PDL experiments for cell adherence: a) 120 nm + lipoic acid +PDL; b) 120 nm +PDL; c) 20 nm +lipoic acid +PDL; d) 20 nm +PDL; e) 120 nm +PDL after 96 hours.

In 120 nm gold coated wafer, cells treated with PDL alone had cell adherence up to 96 hours as shown in the Figure 4.3 e). Cells were adhered by physisorption. Cells adhered due to the electrostatic interaction between the positively charged PDL surface and the negatively charged cell.

In the design of the device, gold was coated over the nanofins as well as the milled region of the contact pad alone. So the main aim was to place a cell just over the gold nanofins. But the above result of PDL coating alone could not achieve this.

For that, immobilization of the cells over the gold nanofins alone by cross linking with covalent bond had to be achieved. So again in the next experiment, in order to find the best material for gold functionalization, three materials were selected: Lipoic acid, Cysteamine and L-cysteine. Cysteamine was purchased from Sigma Aldrich (Item #M9768). L-cysteine was purchased from Sigma Aldrich (Item #W326305) The experiment was done in such a way that wafers were just treated with lipoic acid, cysteamine and cysteine with PDL alone, and then along with combination of PDL and NHS and EDC. EDC was purchased from Sigma Aldrich (Item # E6383). NHS was purchased from Sigma Aldrich (Item #56485). First, 40 nm gold coated substrates were cut into small pieces that will fit into the 24 well plates. They were cleaned by sonicating in acetone and ethanol at 60 degrees for 15 minutes and dried by nitrogen gas. The substrates were immersed in 10mM Lipoic acid, 10mM Cysteamine, 10mM L-cysteine separately each having the volume of 1ml in the wells of the 24 well plate and left for 18 hours for SAM formation. After 18 hours, the chips were taken and washed with ethanol and dried with nitrogen. Then immersed with combination of 75mM EDC, 15mM NHS, and 40mM NaCl, 0.1M MES buffer maintained at PH 6 for crosslinking of SAM layer. After crosslinking, the substrates were immersed in $10 \mu\text{g}/\text{cm}^2$ PDL for 24 hours. After PDL formation cells were seeded.

Cultured PC12 cells that were healthy and having a viability of 96% were taken. They were centrifuged and 24ml of fresh media was added. Then 1 ml of cell suspension with the count of 320,000 cells /ml were added to each of the 24 wells.

After 24 hours, following observations were made. Substrates treated with lipoic acid, cysteamine, L-cysteine along with PDL did not show any adherence. In the lipoic acid, cysteamine and L-cysteine along with EDC and NHS batch, cysteamine treated substrates showed some adherence. The substrates treated with EDC and NHS alone didn't show any adherence. The substrates treated with lipoic acid, cysteamine, L-cysteine along with EDC and NHS and finally treated with PDL showed good level of adherence. Out of the three, cysteamine showed better level of adherence. The cells were not adhered in a regular fashion. Among the controls, just tissue culture plate, the untreated gold substrate did not have any adherence, but the PDL treated structure showed adherence.

Imaging was done after another 48 hours. The result of the experiment was that, the cells were not adhered after 48 hours. So, with cysteamine alone taken since it had better adherence among the 3 chemicals, the experiment was repeated by changing the concentration. But in the SAM formation step, gold coating was dissolved in the cysteamine solution. This may be due to the sonication, which was done for 15 minutes. So the sonication was reduced to 5 minutes and the process was repeated in the following way.

Four gold substrates were immersed in 3.5ml volume 20mM Cysteamine in a single well plate and left for 18 hours in the room temperature for SAM formation. After 18 hours, the chips were taken and washed with ethanol and dried with nitrogen .Then immersed in combination of 150mM EDC, 30mM NHS, and 80mM NaCl, 0.2M MES buffer maintained at PH 6 for crosslinking of SAM layer. After crosslinking, the substrates were immersed in 20 $\mu\text{g}/\text{cm}^2$ PDL

for 24 hours. After PDL formation, cells were seeded. Out of the 24 well plates, 4 of them have the Au substrates treated with cysteamine, EDC and NHS, and PDL. 4 had just PDL and the other 4 were the control substrates, the tissue cultured plates already coated with PDL. 1 ml of cell suspension was added to each of the 12 wells. Results were observed in the next 24 hours.

Cysteamine +EDC NHS+PDL treated substrates had little non uniform adherence as shown in Figure 4.4 b). 3 PDL treated substrates had uniform adherence of PC12 cells as observed in Figure 4.4 a). The fourth one had some adherence. The tissue culture plates had uniform adherence.

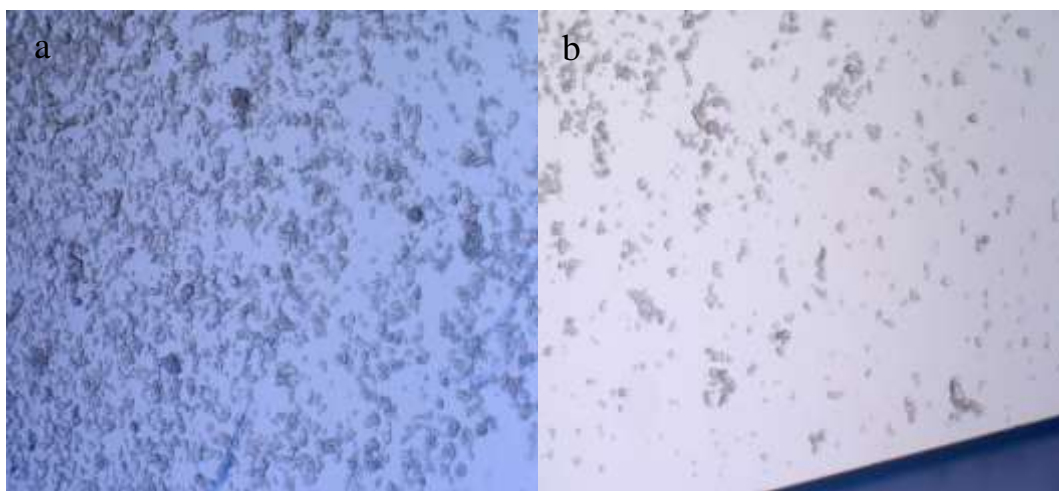


Figure 4.4. Comparing the adherence between PDL and cysteamine: a) PDL; b) cysteamine+EDC NHS+PDL.

From the Figure 4.4, it can be inferred that PDL alone over the substrate showed better adherence. Cysteamine +EDC NHS +PDL treatment is the better choice since it has the cross linking and hence the covalent bond formation but it has to be further investigated. For the adherence of PC 12 cells on the gold substrates using SAM formation and crosslinking by covalent bonding, the following experiment was started. In a six well plate, 2 gold coupons were immersed in 10 mM cysteine and another 2 gold coupons were immersed in 10mM cysteamine

solution. After 12 hours, the samples were observed that gold got peeled off in cysteamine treated coupons.

In order to further investigate the peeling of gold during the cysteamine treatment as well as after fixing the cells, scratch test was done. First the scratch test was performed on the coupons having 10 nm Ti coating followed by 50 nm gold alone. It was concluded that the gold coating was good and the bonding between the gold and the substrate was stronger. But the gold peeling may be due to the thin SiO_2 layer over the Si substrate.

An experiment was started taking the gold chips and immersing them in 10mM cysteamine, 10mM L-cysteine, 100mM L-cysteine. It was observed that gold got peeled off in cysteamine solution. Gold scratch test was done in the cysteine treated and partially dissolved cysteamine treated substrates. So, L-cysteine was selected to be used for SAM formation till the cause for dissolving of gold in cysteamine solution can be found.

4.2.2.3.1 Contact angle measurement. The gold coupons were treated with L-cysteine, EDC NHS and then by PDL and the contact angle was measured in each step. Smaller the contact angle is, more hydrophilic the surface is, and the more adherent the surface is going to be (Hoang et al., 2009). In each step, the contact angle was reduced so that the substrates are conducive for adherence as observed in the Figure 4.5.

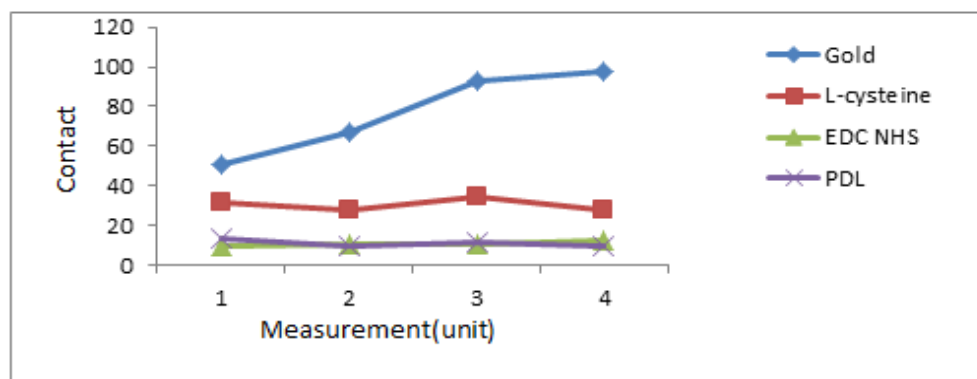


Figure 4.5. Contact angle measurements of the intermediate steps of functionalization.

Finally, the characterization using covalent bonding by EDC NHS crosslinking with MPA and L-cysteine SAMs showed good adherence, which gave positive results.

In this experiment, SAM formation was done by treating the substrates with ethanolic solution of L-cysteine and MPA for 18 hours. In a six well plate, the following combination of MPA (Mercapto propionic acid), L-cysteine, EDC NHS and PDL as shown in the table was done. PC 12 Cells with 560,000cells /ml count and at a viability of 85% was seeded.

Table 4.1.

Six well plate combinations of MPA, L-cysteine

MPA + EDC NHS + PDL	L cysteine + EDC NHS + PDL	L cysteine
MPA + PDL	L cysteine + PDL	MPA

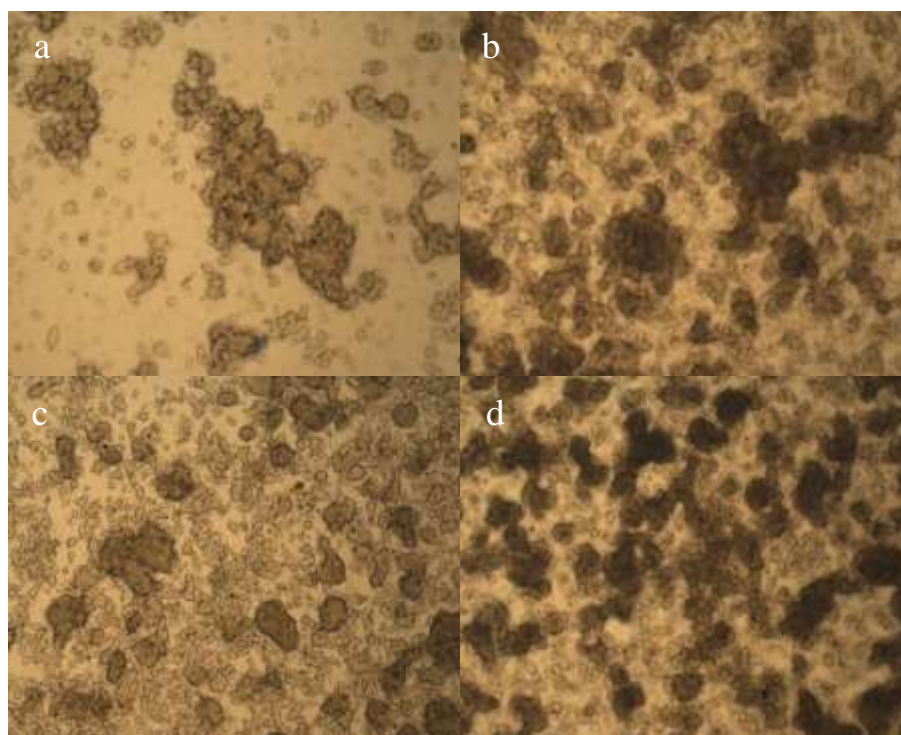


Figure 4.6. Cell adherence after 3 days: a) L-cysteine +EDC NHS +PDL; b) L-cysteine +PDL; c) MPA +EDC NHS +PDL; d) MPA + PDL.

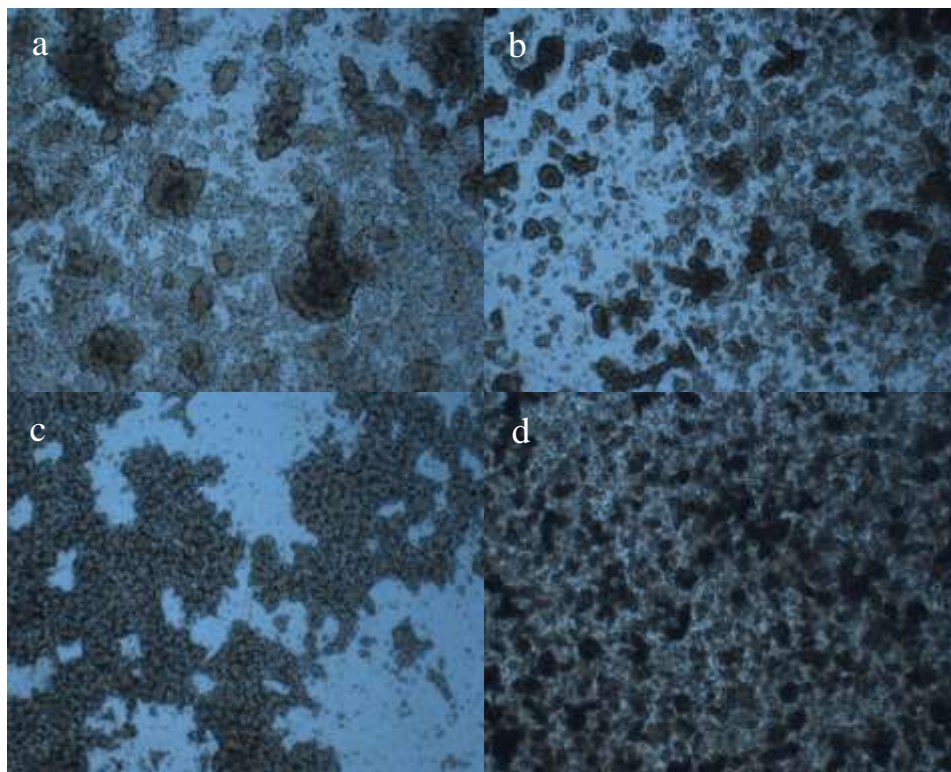


Figure 4.7. Cell adherence after 5 days: a) L-cysteine +PDL; b) L-cysteine+ EDC NHS +PDL; c) MPA+EDC NHS +PDL; d) MPA+ PDL.

Figure 4.6 shows cell adherence on 3rd day for various combination of MPA, EDC NHS and PDL. Figure 4.7 Shows cell adherence on 5th day for various combination of MPA, EDC NHS and PDL. Cells were adhered in all the substrates and they were healthy and growing well and proliferating over the substrates.

4.3 Cell Culturing over Nanofins

In the next stage cells were cultured over the substrates having pillars and nanofins. The gold coated substrates with nano pillars were taken and cleaned by sonicating in ethanol and acetone. Then the substrates were immersed in 0.1 mg/ml of PDL .i.e.0.15 ml PDL+2.85 ml deionized water for twenty four hours.

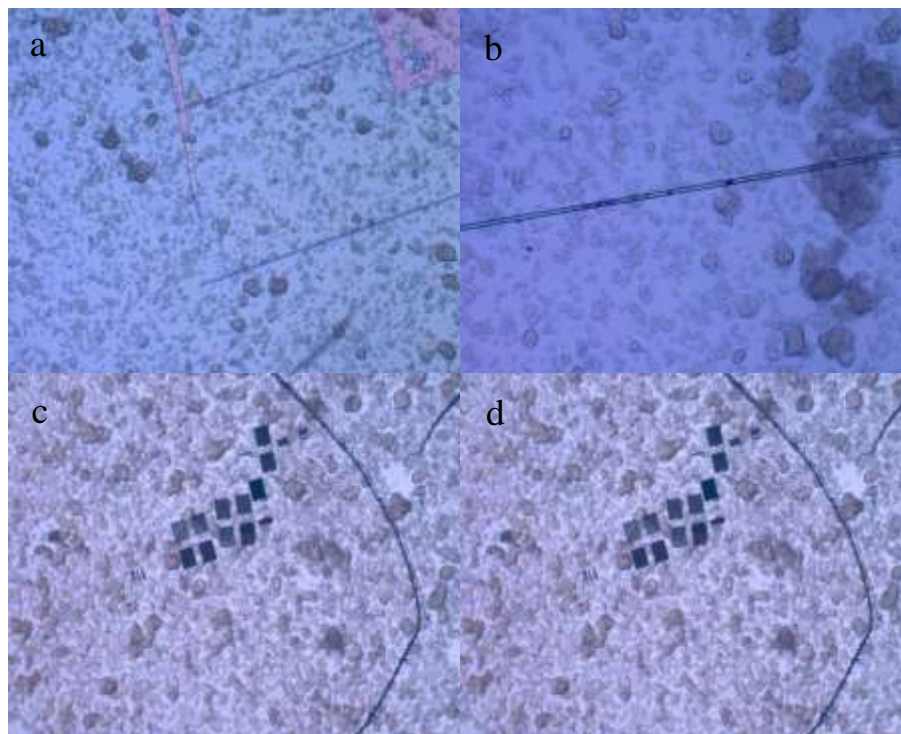


Figure 4.8. ZEISS Z2M upright microscope images of PC 12 cells: a) over nanofins with 5X magnification; b) Over nanofins with 10X magnification c) Over nanofins of $1\mu\text{m} \times 1\mu\text{m}$ area with 10X magnification; d) Over nanofins of $1\mu\text{m} \times 1\mu\text{m}$ area with 20X magnification.

The cells were adhered over the nanofins as well as the high density nanofins of $1\mu\text{m} \times 1\mu\text{m}$ area and the observation was made in ZEISS Z2M imager.

In order to get much clearer image, the substrates were observed under EVO,

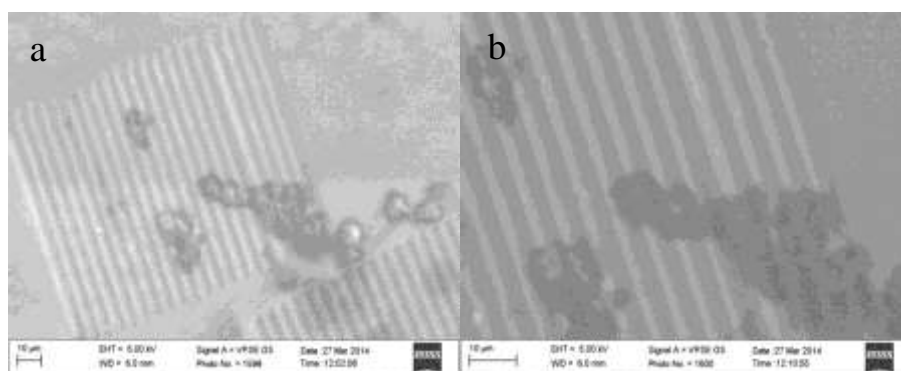


Figure 4.9. EVO SEM images of PC 12 cells over the nanofins: a) Cells over nanofins; b) Magnified image of cells over nanofins.

Since the images clearly didn't show the cells over the nanofins, the next step was to fix them and observe under the Auriga SEM. The experiment was started with PDL with 0.1mg/ml and 0.2 mg/ml of concentration. Two gold coated substrates were cleaned by rinsing with ethanol and acetone. Out of the two substrates, the substrate with gold coated tracks and nanofins was coated with 0.1mg/ml of PDL and the substrate with larger number of nanofins was coated with 0.2 mg/ml of PDL.

Out of the two, the substrate with the concentration of 0.1mg/ml had better uniform adherence. After the cell adherence, the cells were fixed by using the following protocol. The first step was to fix the cells. The substrates were treated with 25% cacodylate, 12.5% paraformaldehyde, 10% gluteraldehyde and 52.5% water. The next step was dehydration. Here the fixed cells were treated with varied concentration of acetonitrile. First the fixed substrates were immersed in 25% acetonitrile for 10 minutes. And then they were immersed in 50% acetonitrile and 50% water for 10 minutes. And then in 75% acetonitrile and 25% water for 10 minutes and 100 % acetonitrile for 10 minutes. The last step was repeated again. Now, the substrates were dried gently with nitrogen gas and were ready for imaging in SEM.

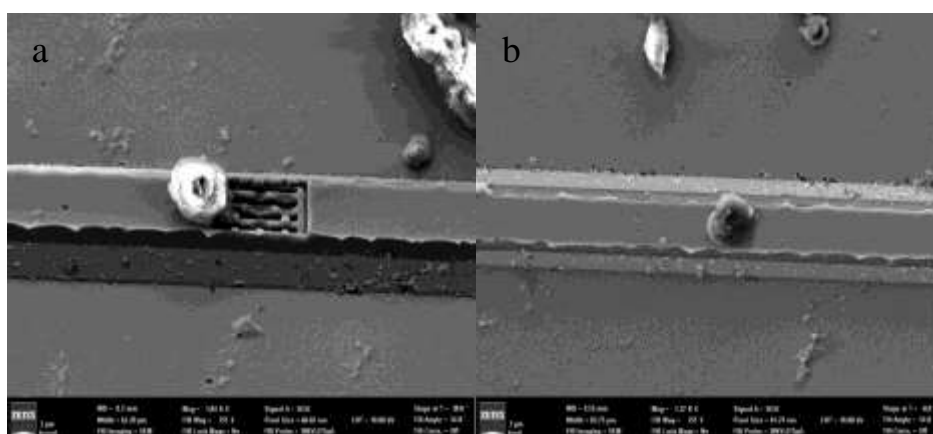


Figure 4.10. SEM images of cell over the track: a) Cell near the nanofins; c) Cell over the track line

From the Figure 4.10, it was observed that the cells were growing on the the track lines and near the nanofins. It was also observed that the pillars were eroded .It may be due to repeated sonication or the cell fixing treatment methods.

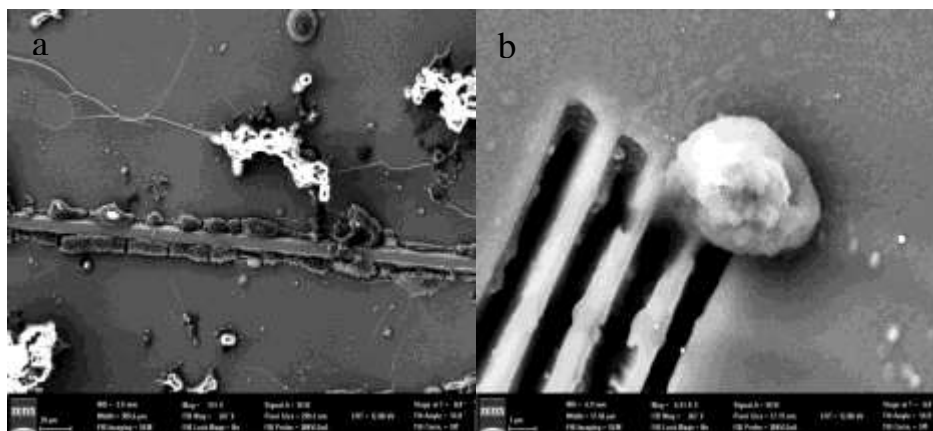


Figure 4.11. SEM images of cell near the track a) Cell near the ridges of the track b) Cell on the edge of the large lines.

The experiment was repeated on a new substrate with nanofins to optimize the cell placement .There were no cells on the nanofins. Cells were clinging to the track lines or lying on the edge of large cut lines as shown in the Figure 4.11. Again the experiment was repeated with one substrate having the track lines and the other Si substrate with high density nanofins.

In order to optimize the placement of the cells over nanofins, adherent A549 cells were selected and cultured over nanofins. Cells were cultured over the substrates having high density pillars as well as nanofins. A reservoir was placed around the pillars using Loctite 5240 silicone light cure adhesive sealant, to culture cells.

A549 cells at a viability of 95%, at seeding density 50,000 cells/ml were seeded on the nanofins contained in the reservoir. After seeding, the cells were incubated for 24 hours to attach. After attachment, the cells were fixed with cacodylate buffer containing formaldehyde and gluteraldehyde and imaged.

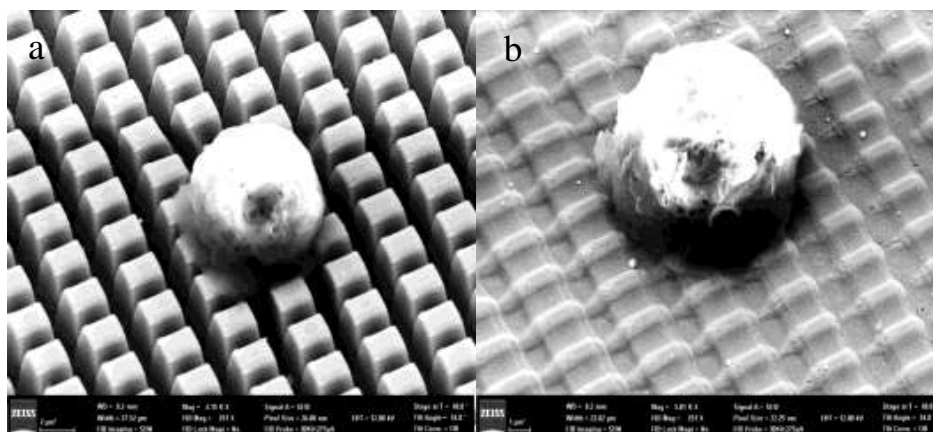


Figure 4.12. Adhered cell over high density nanofins: a) Cell over the pillars; b) Cell over the nanofins.

The cells were able to adhere over the pillars and nanofins as shown in the Figure 4.12. Now, in order to find the optimum condition for the placement of cells over the nanofins, nanofins were milled and A549s were cultured over the nanofins with several placement areas. The well was placed over the area containing the nanofins with a count of $67,500$ cells per well and $125\mu\text{L}$ at 5.5×10^5 cells/ml.

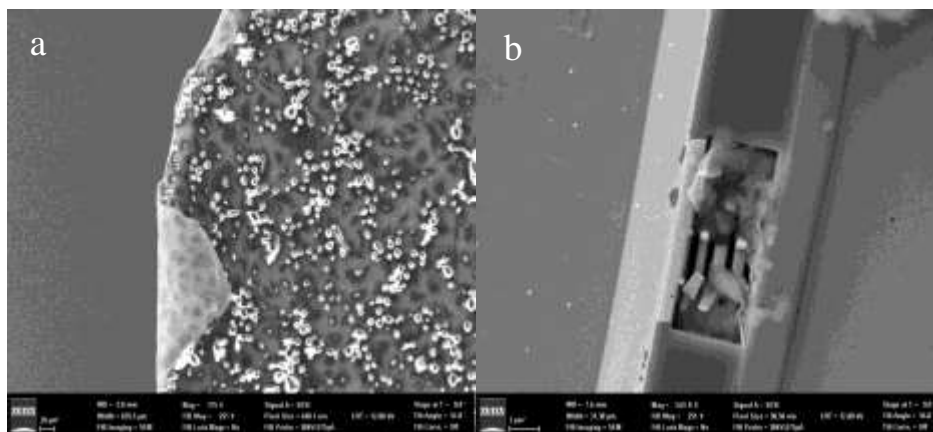


Figure 4.13. SEM images: a) Gold peeling b) Displaced nanofins.

It can be observed that lot of substance covering the whole area within the well and also the gold coating was peeling off as shown in Figure 4.13 a). The nanofins might have been displaced by the thick coating as well as the fixing treatment as shown in the Figure 4.13 b).

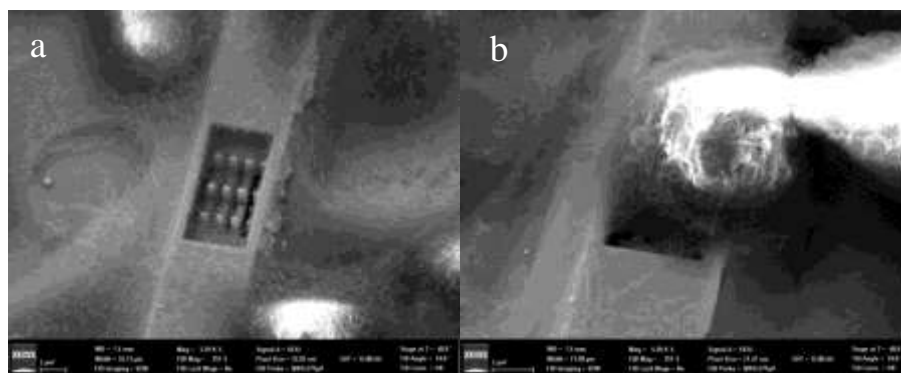


Figure 4.14. Adhered cells over low density nanofins: a) Placement chamber; b) Cell over the placement chamber.

The cells were able to adhere over the nanofins in the placement chamber as shown in the Figure 4.14 b).

4.4 Differentiation Experiments

Cells were seeded at a density of 10,000 cells per well in a 24 well plate. They were allowed to grow for 24 hours after which media containing nerve growth factors (NGF). NGF obtained from Corning (Item # 354005) was added to cells at 2 different concentration viz. 50 and 100ng/ml. The media was changed every other day.

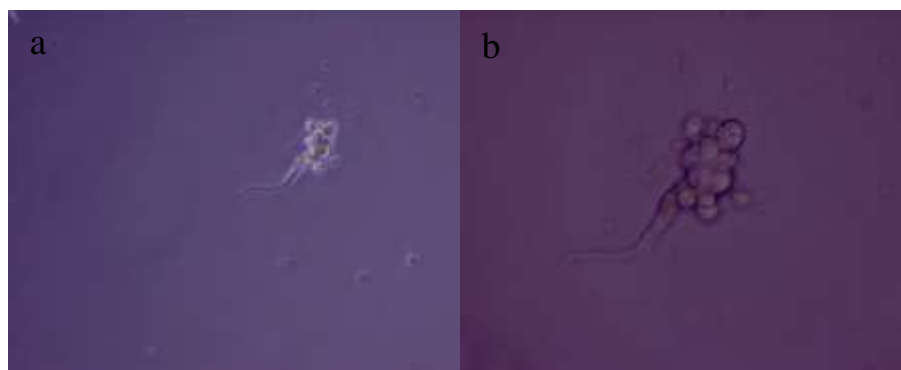


Figure 4.15. Differentiated PC12 cells: a) 20X magnification b) 40X magnification

Observations were made when changing the media. One neuron was shown to differentiate after 7 days for 100ng/ml as shown in the Figure 4.15

After this result was obtained, another experiment with 3 different concentrations was started. The concentration selected this time was 100, 150 and 200ng/ml. Two sets of experiments were incorporated within, one where media was premixed with NGF and the other being adding NGF directly to wells with media. Media was changed every other day. Third set of experiment was included where cells were allowed to grow for 48 hours after they were seeded before NGF's was added.

Table 4.2.

Combination of NGF Concentration in ng/ml

Cntrl (media + NGF)	Cntrl (NGF)	Cntrl (NGF)
Cells adhered for 24 hours before NGF is added		48 hours
100	100	100
150	150	150
200	200	200



Figure 4.16. Cell adherence on 1st day

With low density seeding, cells were adhered with space in-between, conducive for differentiation as shown in Figure 4.16.

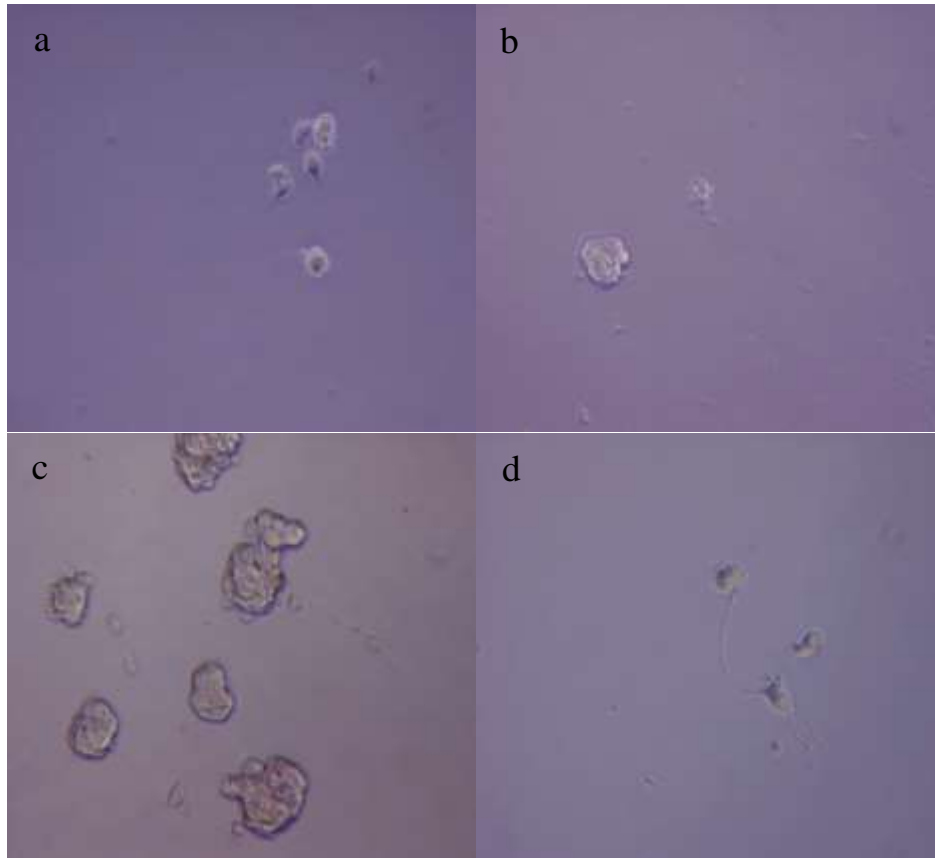


Figure 4.17. Differentiation on: a) 3rd day; b) 5th day; c) 6th day; d) 6th day of adding NGF.

Observations were made when media was changed .Differentiation started on 2nd day .Lot of differentiated cells were found on 6th day. On 6th day, neurite outgrowths were shown many differentiated cells .In some cases, two neurons were communicating as one neurite extension reached the other PC 12 cell as shown in the Figure 4.16 d).

4.5 Preliminary Impedance Measurement

The device consists of contact pads and track lines to make electrical connections. After fabrication of the device, a well was sealed over the area that has the nanofins .The output was taken from the contact pad by drawing contact lines using conducting glue and then by placing a conducting wire.

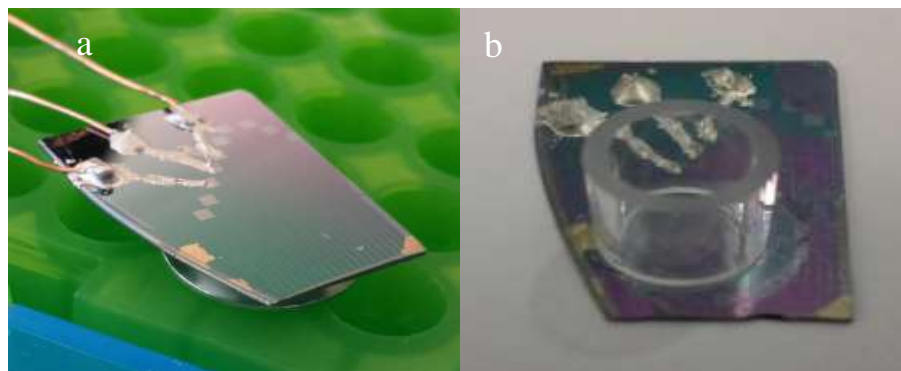


Figure 4.18. Device setup for impedance measurement: a) Device with output taken from the contact pads by conducting glue and copper wire b) Device and the sealed well.

The impedance was measured using the potentiostat. The impedance was measured between the conducting wire and the reference platinum electrode placed inside the medium. The measurement was taken from 4000-100 Hz at amplitude of 40 mV and 50 points per decade.

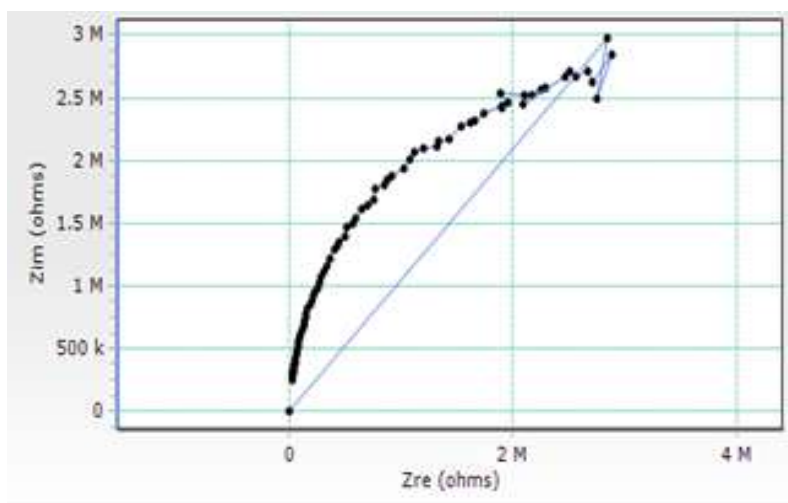


Figure 4.19. Impedance measurement.

In the nyquist plot, the real part of the impedance vector was plotted on the X axis and the imaginary part on the Y axis as shown in Figure 4.18. Reference reading was taken. The impedance value was very high deviating from the impedance posed by the cell and so no conclusion was made. Further electrical readings should be taken in future experiments.

CHAPTER 5

Discussion and Future Research

5.1 Device Fabrication

Device was fabricated with Si conducting lines and contact pads completely insulated by SiO_2 layer and gold coated nanofins as shown in Figure 5.1. Standard photolithographic technique was followed for industry compliance. Interfacial impedance and electrode resistance issues were addressed in the improved nanofin design. Large surface area can reduce interfacial impedance and large cross section area can reduce the electrode resistance. But this statement has to be further proved theoretically as well as experimentally.

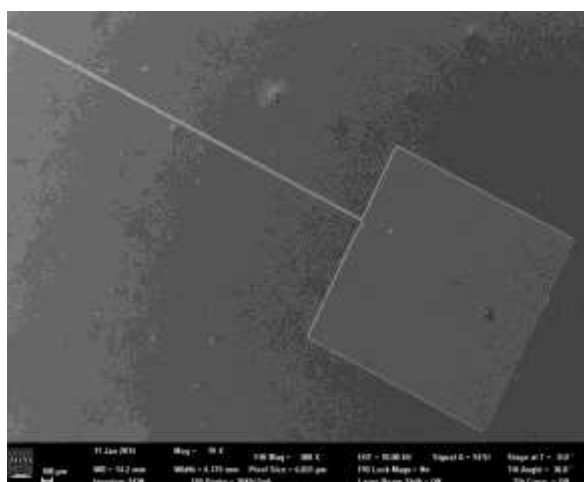


Figure 5.1. Device with contact pad and track lines.

Device consists of conducting lines and contact pad as shown in the Figure 5.1. Output was taken from the contact pads by conducting glue and copper wire. Fully functional device will be fabricated in the future research work.

In the SOI based process flow, Al lift off was performed so that gold remains only over the nanofins. This design enables cell placement by gold functionalization. But gold etching caused some erosion in the nanofins. Further optimization of the process flow should be done to

improve the design. Also elemental analysis should be conducted to optimize and confirm gold deposition over nanofins. In SEM, Energy dispersive X-Ray spectroscopy can be used for elemental analysis.

5.2 Nanofin Fabrication

Nanofins of width 200nm were fabricated using Focused Ion Beam. First, 200nm width was achieved by optimizing the current to 275 pA. Then ideal height was achieved by optimized dosage of 10nC.

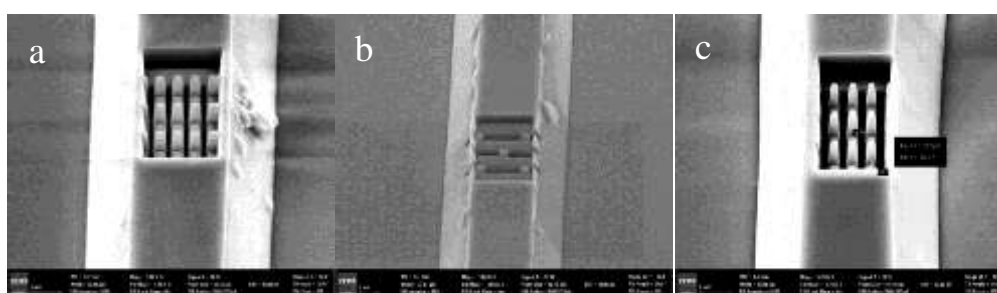


Figure 5.2. Nanofin structures with a) 10 nC; b) 5 nC; c) 10 nC Dosages.

Nanofin dimensions were optimized and various nanofin structures were milled for growth and proliferation of PC12 cells as shown in Figure 5.2. The above mentioned optimization was done keeping the acceleration voltage of SEM at 30 KV. If this voltage setting is changed to 15 KV, with the lower current values in the order of pA, lower width nanofins in the order of 100nm to 50nm nanometer can be milled.

5.3 Cell Culture over Nanofins

A reservoir was placed around the nanofins using bio compatible sealant, to culture cells. A549 cells were seeded on the pillars and nanofins contained in the reservoir and incubated to attach. After attachment, the cells were fixed and imaged in FESEM. Cells were successfully cultured over the high density and low density nanofins.

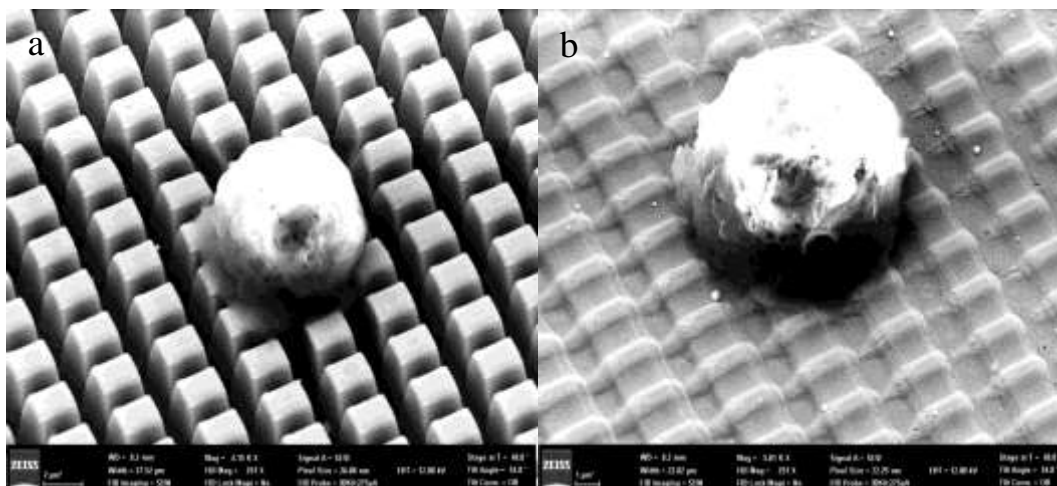


Figure 5.3. Cell cultured over high density a) Pillars; b) Nanofins.

The penetration of cells over high density pillars and nanofins was a challenge as they exhibit the bed of nail phenomenon as shown in Figure 5.3. But comparatively nanofin penetration was easier. In future work, density of nanofins should be optimized for better internalization.

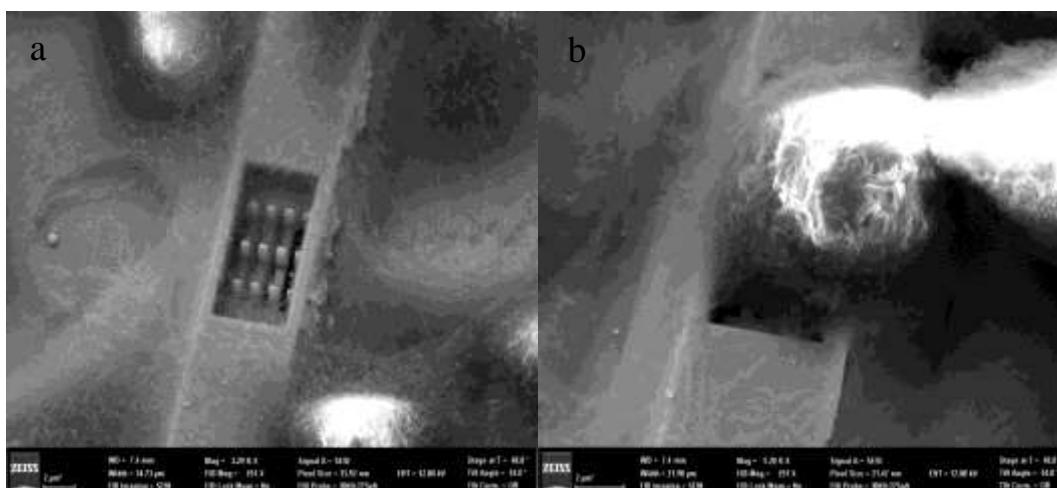


Figure 5.4. Cell cultured over high density nanofins : a) Placement chamber; b) Cell adhered over nanofins.

Cells were adhered over low density nanofins. Here the internalization of cells was easier compared to high density nanofins. Placement procedures were optimized for better cell

adherence. Both high density and low density seeding of cells were studied. For adherence, large seeding density was considered for better chance of adherence. Cell adherence by immobilization technique should be implemented in future work for optimized cell placement.

5.4 Immobilization of Cells over Gold Surfaces

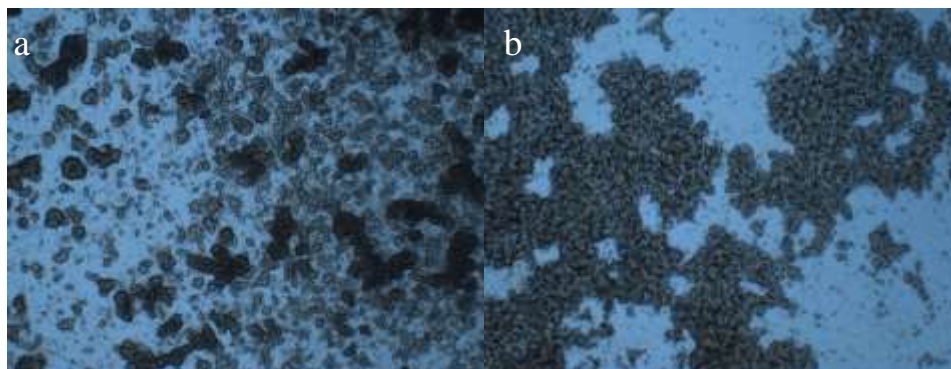


Figure 5.5. Adherence of PC12 cells by chemisorption: a) L-cysteine+ EDC NHS +PDL; b) MPA+EDC NHS+PDL.

Gold functionalization protocol was fine tuned to immobilize cells for longer time by means of covalent cross linking. Both MPA and L-cysteine SAMs with EDC NHS cross linking and PDL combination worked successfully as shown in Figure 5.5. Concentration and P_H was optimized to get better adherence. The cells were able to adhere successfully for 5 days.

Even though contact angle measurement gave a good indication, further AFM imaging and analysis should be performed to confirm the SAM formation and cross linking chemistry.

5.5 Differentiation



Figure 5.6. Differentiation of PC12 cells.

PC 12 cells were successfully differentiated to neurons. Neurites were extending from the cells connecting them as shown in the Figure 5.6. Success of differentiation depends on NGF concentration, seeding density. NGF concentration of 200 ng/ml and Lower density of 10,000 cells per ml were the optimized values.

5.6 Future Research

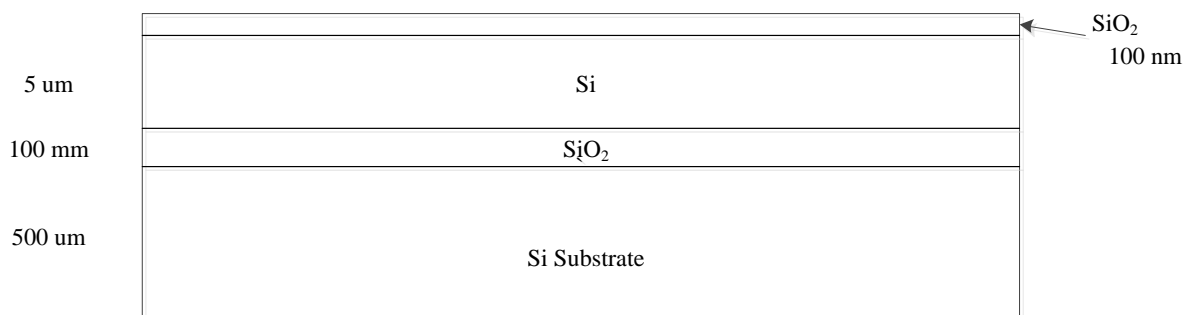
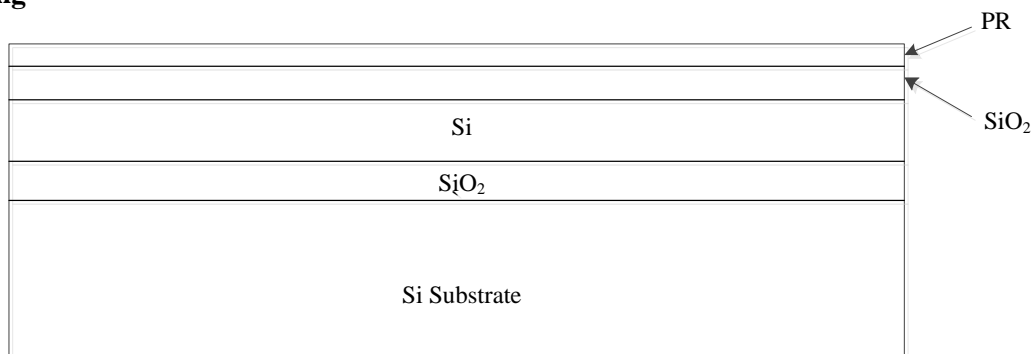
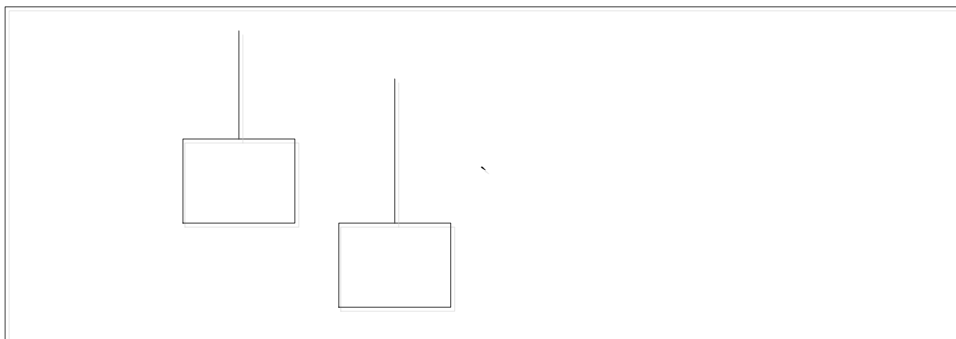
In this research, a nanodevice with 200 nm nanofins was designed and fabricated successfully. For nanofin cell interfacing, adherence protocol for PC12 cells and differentiation protocol was optimized. Now with these results, the next step is to optimize the cell placement protocol to interface the PC12 cells over the nanofins and differentiating them to neurons. The design of the device is such that gold is coated only over the nanofins. Since the immobilization of PC12 cells with covalent cross linking was optimized, the placement of the cells over the nanofins can be achieved easily. If placement protocol is further optimized, it opens up lot of possibilities for future research. Electrical studies and intracellular recording with model PC12 cell lines can be continued. In this context, the nanofin dimensions and density can be optimized for neuronal cell growth, proliferation, mobility and differentiation. Apart from these, cell placement and growth protocol can be established for more realistic cell systems like rat cortical neurons and cardiomyocytes over nanofins. In the long run, research options include monitoring and stimulation of neuronal network events, drug delivery and single cell imaging.

References

- Brüggemann, D., Wolfrum, B., Maybeck, V., Mourzina, Y., Jansen, M., & Offenhäusser, A. (2011). Nanostructured gold microelectrodes for extracellular recording from electrogenic cells. *Nanotechnology*, 22(26), 265104.
- Carlson, N. (2005). *Foundations of Physiological Psychology* Allyn and Bacon: Boston.
- Eschermann, J. F., Stockmann, R., Hueske, M., Vu, X. T., Ingebrandt, S., & Offenhausser, A. (2009). Action potentials of HL-1 cells recorded with silicon nanowire transistors. *Applied Physics Letters*, 95(8), 083703-083703-083703.
- Fujita, T. (1976). Concept of paraneurons. *Archivum histologicum Japonicum= Nihon soshikigaku kiroku*, 40, 1-12.
- Hai, A., Shappir, J., & Spira, M. E. (2010). In-cell recordings by extracellular microelectrodes. *Nature methods*, 7(3), 200-202.
- Hoang, T., Ho, L., Swertfager, K., Gill, A., Malhotra, K., Jones, C., . . . Meng, E. (2009). Surface Treatment Strategies for Microfluidic Devices Towards Longitudinal PC12 Neuronal Cell Studies. *Microtechnologies in Medicine and Biology, Quebec City, Canada*, 212-213.
- Jobling, D., Smith, J., & Wheal, H. (1981). Active microelectrode array to record from the mammalian central nervous system in vitro. *Medical and biological engineering and computing*, 19(5), 553-560.
- Kandel, E. R., Schwartz, J. H., & Jessell, T. M. (2000). *Principles of neural science* (Vol. 4): McGraw-Hill New York.
- Kipke, D. R., Vetter, R. J., Williams, J. C., & Hetke, J. F. (2003). Silicon-substrate intracortical microelectrode arrays for long-term recording of neuronal spike activity in cerebral

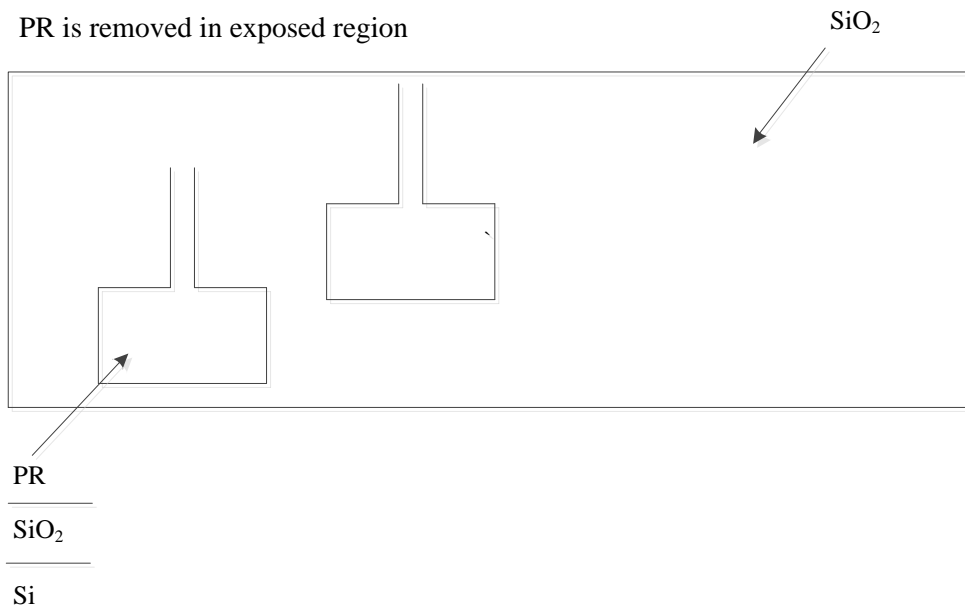
- cortex. *Neural Systems and Rehabilitation Engineering, IEEE Transactions on*, 11(2), 151-155.
- Lennard-Jones, J. (1932). Processes of adsorption and diffusion on solid surfaces. *Trans. Faraday Soc.*, 28, 333-359.
- Love, J. C., Estroff, L. A., Kriebel, J. K., Nuzzo, R. G., & Whitesides, G. M. (2005). Self-assembled monolayers of thiolates on metals as a form of nanotechnology. *Chemical Reviews*, 105(4), 1103-1170.
- Mandel, G., Cooperman, S. S., Maue, R. A., Goodman, R. H., & Brehm, P. (1988). Selective induction of brain type II Na⁺ channels by nerve growth factor. *Proceedings of the National Academy of Sciences*, 85(3), 924-928.
- Martina, M., Luk, C., Py, C., Martinez, D., Comas, T., Monette, R., . . . Mealing, G. A. (2011). Recordings of cultured neurons and synaptic activity using patch-clamp chips. *Journal of neural engineering*, 8(3), 034002.
- Nam, Y., Chang, J. C., Wheeler, B. C., & Brewer, G. J. (2004). Gold-coated microelectrode array with thiol linked self-assembled monolayers for engineering neuronal cultures. *Biomedical Engineering, IEEE Transactions on*, 51(1), 158-165.
- Pine, J. (1980). Recording action potentials from cultured neurons with extracellular microcircuit electrodes. *Journal of Neuroscience Methods*, 2(1), 19-31.
- Robinson, J. T., Jorgolli, M., Shalek, A. K., Yoon, M.-H., Gertner, R. S., & Park, H. (2012). Vertical nanowire electrode arrays as a scalable platform for intracellular interfacing to neuronal circuits. *Nature nanotechnology*, 7(3), 180-184.

- Rudy, B., Kirschenbaum, B., & Greene, L. (1982). Nerve growth factor-induced increase in saxitoxin binding to rat PC12 pheochromocytoma cells. *The Journal of Neuroscience*, 2(10), 1405-1411.
- Schreiber, F. (2000). Structure and growth of self-assembling monolayers. *Progress in surface science*, 65(5), 151-257.
- Spira, M. E., & Hai, A. (2013). Multi-electrode array technologies for neuroscience and cardiology. *Nature nanotechnology*, 8(2), 83-94.
- Thomas, C., Springer, P., Loeb, G., Berwald-Netter, Y., & Okun, L. (1972). A miniature microelectrode array to monitor the bioelectric activity of cultured cells. *Experimental cell research*, 74(1), 61-66.
- Tischler, A. S., Lee, Y. C., Costopoulos, D., Slayton, V. W., Jason, W. J., & Bloom, S. (1986). Cooperative regulation of neurotensin content in PC12 pheochromocytoma cell cultures: effects of nerve growth factor, dexamethasone, and activators of adenylate cyclase. *The Journal of Neuroscience*, 6(6), 1719-1725.
- Xie, C., & Cui, Y. (2010). Nanowire platform for mapping neural circuits. *Proceedings of the National Academy of Sciences*, 107(10), 4489-4490. doi: 10.1073/pnas.1000450107
- Yeh, J. I., & Shi, H. (2010). Nanoelectrodes for biological measurements. *Wiley Interdisciplinary Reviews: Nanomedicine and Nanobiotechnology*, 2(2), 176-188.
- Yuste, R. (2008). Circuit neuroscience: the road ahead. *Frontiers in neuroscience*, 2(1), 6.

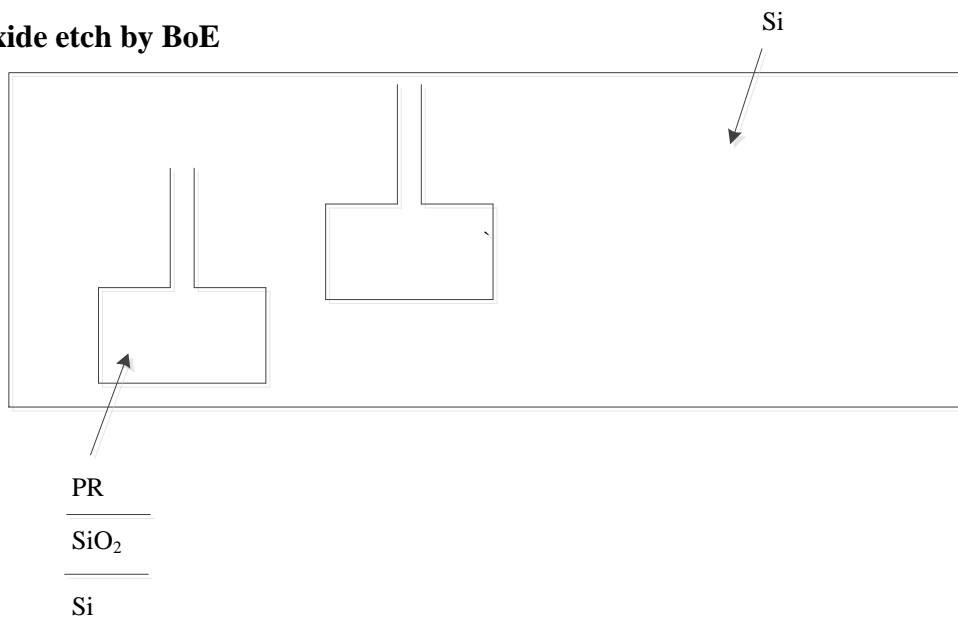
*Appendix A***Process flow Diagram:****1. Oxidation****2. PR Spinning****3. Exposure to UV**

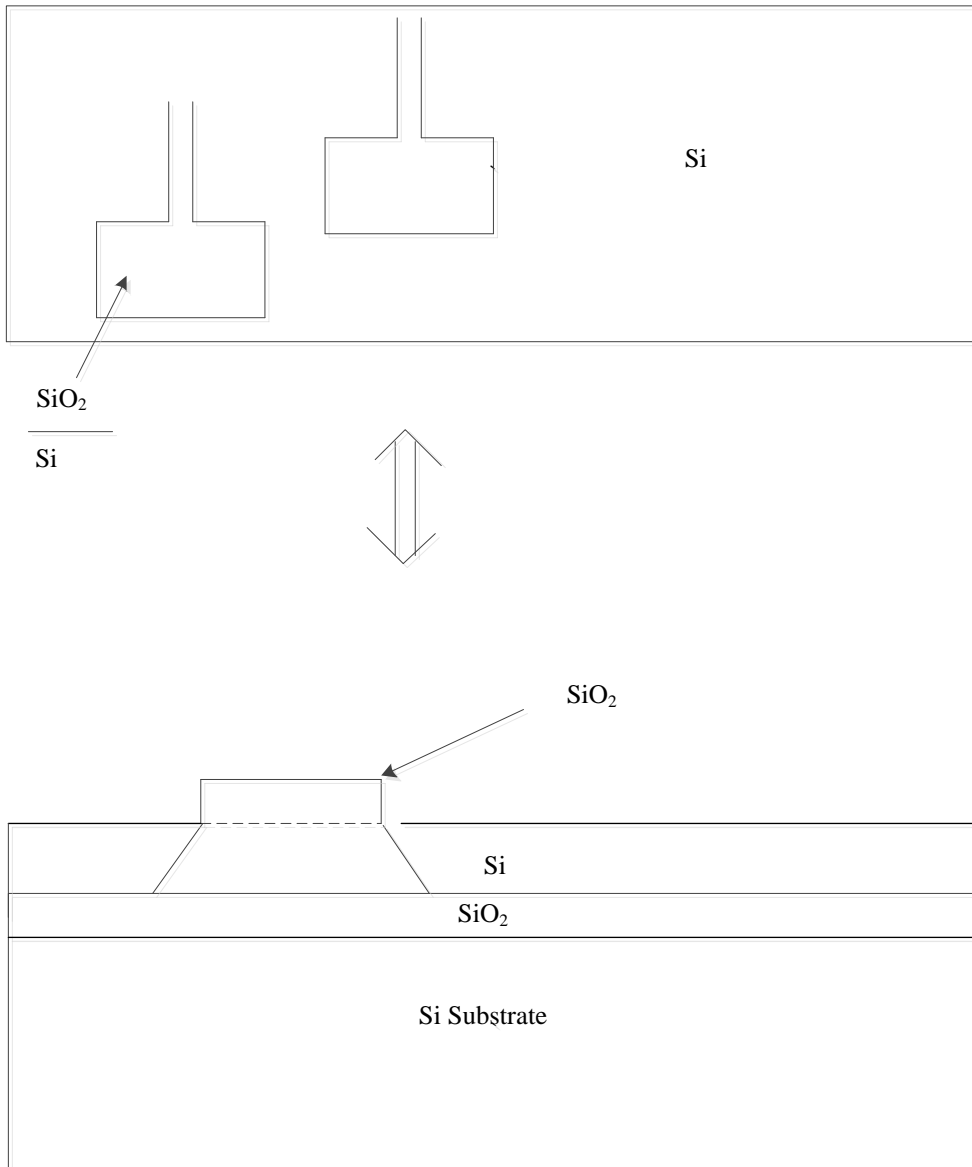
4. Develop

PR is removed in exposed region

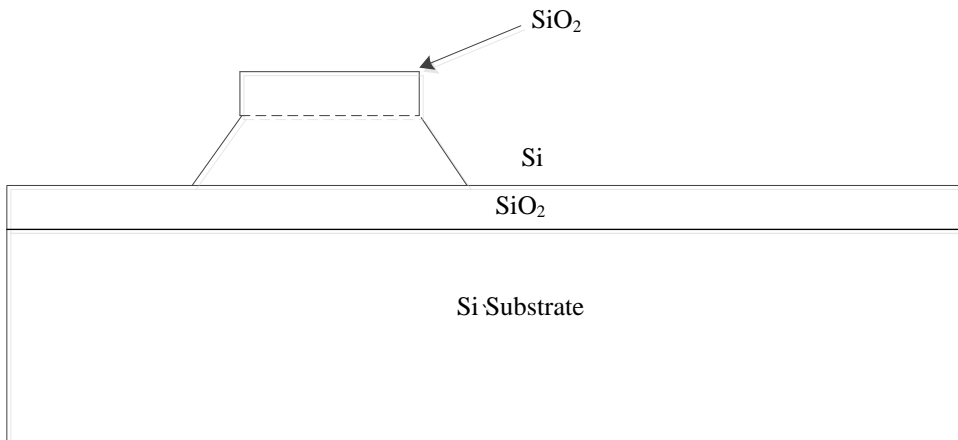


5. Oxide etch by BoE

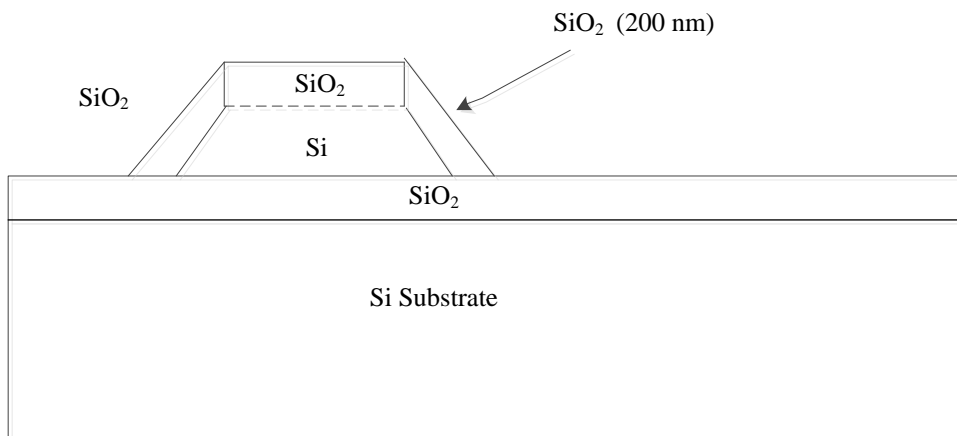


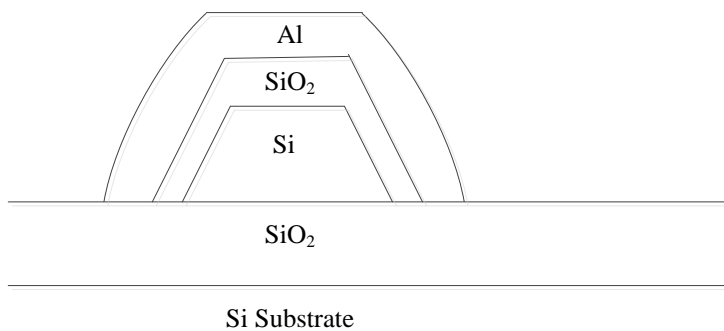
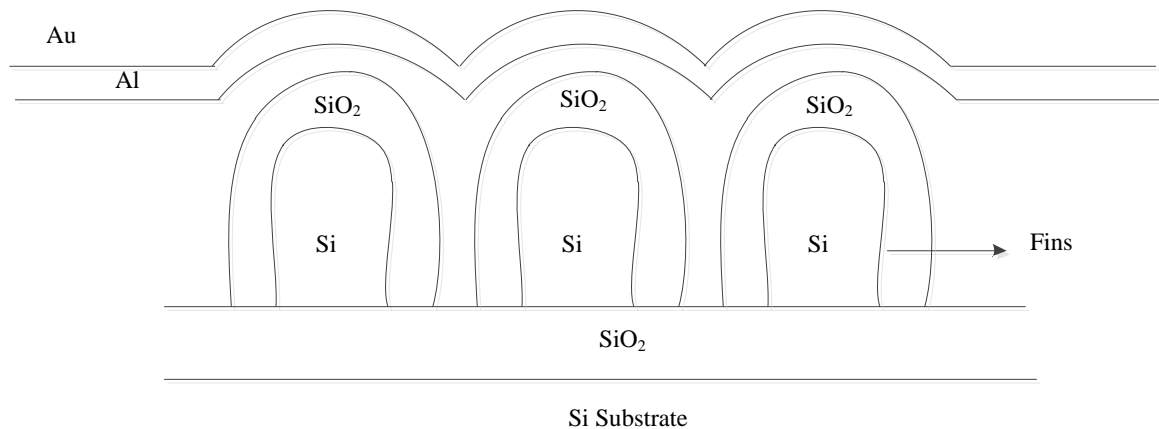
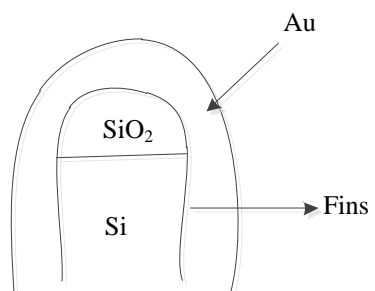
6. PR removed by acetone / IPA

7. Silicon Etch By KOH



8. Oxidation



9. Al deposition**10. FIB . Au Dep****11. Al Etch removes gold everywhere except on Fins**

Appendix B

Process flow steps

These are the detailed steps that are followed in making the device.

- The SOI wafer was first oxidized by dry oxidation.
- O₂ purge was done at 1000 C for 1.5hrs to achieve the targeting oxidation of 60 nm
- Clean by 1:1:5 NH₄OH H₂O₂ H₂O
- Spin coating in the PR spinner
- HDMS which act as glue
- PR S1813
- Soft bake at 95 C
- Align and expose to UV light for 7 seconds
- Develop using MF TM -321
- Soft bake at 95 C
- Oxide wet etch by using BOE(10:1)
- PR is removed by treating with acetone and IPA.
- Si etch is done by 15% KOH
- Again oxidation is done.
- And then, Al is coated using PVD technique.
- Then nanofins are milled.
- And then Au is coated.
- And then Al lift off is done using Al etch so that gold remains only on the nanofins.

*Appendix C***Gold Functionalization protocol**

- Cleaning the substrates: Sonicate gold substrates (50-100 nm thickness) for 15 minutes each in acetone and ethanol.
- SAM formation: Immerse the cleaned gold substrates in 10 mM solution of
- L-cysteine/cysteamine/lipoic acid, in ethanol for 4-6 hours at 40 °C or for 18-24 hours at room temperature.
- Rinse the substrates with ethanol and dry the substrates using nitrogen gas (if there is gap going to the next step, store in substrates in ethanol).
- Immobilization of PDL on SAM-modified gold substrate:
- Activation: Immerse the SAM-modified substrates in 1:1 v/v solution of 0.4 M EDC and 0.1 M NHS in 0.1 M MES buffer at pH 6 for 2 hours.
- PDL formation: Immerse the substrates in 0.5 mg/mL solution of PDL in 10 mM borate buffer at pH 8.5.
- Clean the substrates with ethanol and dry gently using nitrogen gas.
- Rinse the substrates thoroughly with PBS before seeding cells.

*Appendix D***Differentiation Protocol**

- The cells were filtered before seeding.
- The cells were seeded at a density of 10,000 cells /well (can go up to 15,000 cells)
- Then the cells are kept in incubator for 24 hours to adhere.
- Next day, NGF was added (100,150,200 ng/ml concentration) directly to the media. Out of which, 200 ng/ml worked best.
- Next day, media was changed (80% new, 20% old).
- From now onwards, media was changed and NGF was added on alternate days.